

**SEMI-ANALYTICAL FINITE ELEMENT
MODELING FOR DISPERSION ANALYSIS OF
MULTILAYERED STRUCTURES**

**A Thesis Submitted to
the Graduate School of Engineering and Sciences of
İzmir Institute of Technology
in Partial Fulfillment of the Requirements for the Degree of**

MASTER OF SCIENCE

in Mechanical Engineering

**by
Çağrı Gökhan AKYOL**

**July 2017
İZMİR**

We approve the thesis of **Çağrı Gökhan AKYOL**

Examining Committee Members:

Assist. Prof. Dr. Ünver ÖZKOL

Department of Mechanical Engineering, İzmir Institute of Technology

Prof. Dr. Bülent YARDIMOĞLU

Department of Mechanical Engineering, İzmir Institute of Technology

Assoc. Prof. Dr. Abdullah SEÇGİN

Department of Mechanical Engineering, Dokuz Eylül University

31 July 2017

Assist. Prof. Dr. Ünver ÖZKOL

Supervisor,
Department of Mechanical Engineering,
İzmir Institute of Technology



Dr. Onursal ÖNEN

Co-Advisor,
ASELSAN A.Ş

Prof. Dr. Metin TANOĞLU

Head of the Department of
Mechanical Engineering

Prof. Dr. Aysun SOFUOĞLU

Dean of the Graduate School
of Engineering and Sciences

ACKNOWLEDGEMENTS

I would like to express my deepest gratitude to my advisor, Assist.Prof.Dr.Ünver ÖZKOL and Dr.Onursal ÖNEN for their guidance, motivation, support and encouragement during my thesis.

I am especially grateful to my colleagues, Yusufcan UZ, Okan BOSTAN and Cevahir KARAGÖZ for their support, assistance and to make this study more fun.

Special thanks to my committee members Prof.Dr.Bülent YARDIMOĞLU and Assoc.Prof.Dr.Abdullah SEÇGİN for sharing their knowledges, and giving helpful suggestions regarding my thesis studies.

I would also like to thanks to my friends Mehmet Ali AKKAŞ and Nisanur İLHAN for their incredible help and support during this study.

Finally, I am deeply grateful to my family for their continuous support, unlimited patience and love throughout my life.

ABSTRACT

SEMI ANALYTICAL FINITE ELEMENT MODELING FOR DISPERSION ANALYSIS OF MULTILAYERED STRUCTURES

Ultrasonic guided waves are frequently employed for Non-destructive tests (NDT), and Structural Health Monitoring (SHM) applications in the industry. Several analytical and numerical approaches have been developed in order to investigate guided wave behavior on multilayered structures.

In this thesis, guided waves were investigated using the Semi-Analytical Finite Element (SAFE) approach on planar (plate like) structures. The guided wave theory and dispersive behavior in bounded structure were presented for Lamb waves for isotropic elastic plate model first. The numerical method to solve the SAFE problem was developed using the Matlab 2014b in order to obtain dispersion curves. The curves were compared with the Disperse Software, which utilizes global matrix approach for analytical solution of the same problem. Good agreement was achieved on obtained dispersion curves.

As a second part of this study, dispersion analysis was carried out in a multi-layer plate model consisting of elastic and viscoelastic materials. The semi-analytical finite element method was solved by adapting the hysteretic damping model so that it can also be applied in a damped plate model. Phase velocity and attenuation dispersion curves were illustrated and the effect of the viscoelastic layer thickness is also discussed. The obtained attenuation dispersion curves in this damped plate configuration are examined for wave modes with low-attenuation. The dispersion curve results obtained using the SAFE method was also compared with the results of studies available in literature.

ÖZET

ÇOK KATMANLI YAPILARIN BOZUNMA ANALİZİ İÇİN YARI-ANALİTİK SONLU ELEMAN MODELLEMESİ

Ultrasonik yönlendirilmiş dalgalar, endüstrideki Tahribatsız Muayene (NDT) ve Yapısal Sağlık İzleme (SHM) uygulamaları için sıklıkla kullanılır. Çok katmanlı yapılarda yönlendirilmiş dalga davranışını araştırmak için çeşitli analitik ve sayısal yaklaşımlar geliştirilmiştir.

Bu tez çalışmasında, plaka benzeri yapılar üzerinde Yarı-Analitik Sonlu Elemanlar yaklaşımıyla yönlendirilmiş dalgalar araştırılmıştır. Öncelikle, sınırlı yapılarda ki yönlendirilmiş dalga teorisi ve dispersiyon (bozunma) davranışı, izotropik elastik plaka modeli üzerinde Lamb dalgaları göz önüne alınarak sunulmuştur. Dispersiyon eğrileri elde etmek için, SAFE probleminin sayısal çözümleri Matlab 2014b programı kullanılarak geliştirilmiştir. Dispersiyon eğrileri, aynı sorunun analitik çözümü için global matris yaklaşımını kullanan Disperse programı ile karşılaştırılmıştır. Bu karşılaştırma sonucunda, dispersiyon eğrileri üzerinde elde edilen değerlerde iyi bir mutabakat sağlandığı görülmüştür.

Bu çalışmanın ikinci bir parçası olarak, elastik ve viskoelastik malzemelerden oluşan çok katmanlı plaka modelinde dispersiyon analizi yapılmıştır. Yarı-Analitik Sonlu elemanlar metodu, sönümlü plaka modelinde uygulanabilmesi için Histeretik sönümlenme modeli adapte edilerek çözülmüştür. Faz hızı ve zayıflama dispersiyon eğrileri olarak gösterilmiş ve viskoelastik yapının etkileri tartışılmıştır. Bu sönümlü plaka konfigürasyonundan elde edilen zayıflama dispersiyon eğrileri düşük zayıflamaya sahip dalga modu seçimi için incelenmiştir. SAFE yöntemi kullanılarak elde edilen dispersiyon eğrisi sonuçları, literatürde mevcut olan çalışmaların sonuçları ile de karşılaştırılmıştır.

TABLES OF CONTENTS

LIST OF FIGURES	viii
LIST OF TABLES.....	ix
LIST OF SYMBOLS	x
CHAPTER 1. INTRODUCTION	1
CHAPTER 2. LITERATURE SURVEY.....	5
2.1 Guided Acoustic Waves in Solids.....	5
2.2 Modeling Guided Acoustic Waves	6
2.2.1 Analytical Modeling	6
2.2.2 Finite Element Modeling	9
2.3 Semi Analytical Finite Element Modeling.....	11
2.3.1 SAFE for Modeling of Guided Waves	12
CHAPTER 3. FUNDAMENTALS OF GUIDED WAVES.....	15
3.1 Bulk Waves in Isotropic Media.....	15
3.1.1 Equation of Motion.....	15
3.1.2 Helmholtz Decomposition method	17
3.1.3 Bulk Longitudinal and Shear wave velocities	19
3.2 Guided Wave in Isotropic Media	20
3.2.1 Phase and Group Velocity	27
3.2.2 Modes and Mode Shapes	31
CHAPTER 4. SEMI-ANALYTICAL FINITE ELEMENT METHOD	34
4.1 Definition of SAFE Method for Guided Waves	34
4.2 Hamilton's Principle	38
4.3 Post Processing of Eigenvalue Problem.....	43
4.3.1 Group Velocity Concept	45

CHAPTER 5. SAFE METHOD NUMERICAL EXAMPLES	47
5.1 Case Study-1	48
5.1.1 Results.....	48
5.2 Case Study-2	52
5.2.1 Results.....	55
5.3 Case Studies-3.....	57
CHAPTER 6 DISCUSSION AND CONCLUSION	62
6.1 Future Work	63
REFERENCES	65

LIST OF FIGURES

<u>Figure</u>	<u>Page</u>
Figure 1.1. Comparison of Bulk wave and Guided wave inspection techniques	2
Figure 1.2. Application of SAFE method for planar structures	3
Figure 3.1. Guided wave plate model for isotropic elastic bounded medium with the directions (x_1, x_2, x_3)	20
Figure 3.2. Symmetric and Antisymmetric wave modes representation on plate	23
Figure 3.3. Frequency-Wavenumber dispersion curve of 1-mm thickness Aluminum plate	27
Figure 3.4. Group velocity and Phase velocity representation	28
Figure 3.5. Phase velocity dispersion curve of 1-mm Aluminum Plate model	29
Figure 3.6. Group velocity dispersion curve of 1-mm Aluminum plate.....	31
Figure 3.7. Wave structure for different points on S_0 and A_0 wave mode of Aluminum plates with in plane displacement (u , solid line) and out- of plane displacement (w , dashed line).....	32
Figure 4.1. Representation of infinitely long plate model in (y) direction with discretization on the plate thickness with 2 quadratic line elements (a), Degrees of freedom for each displacement and direction (b), At each elements individual location of isoparametric element (c).....	35
Figure 5.1. Phase velocity Dispersion curve of 2-mm thickness titanium plate structure results for SAFE (a) and for GMM (b).Red line for symmetric modes, blue line for asymmetric wave modes.	49
Figure 5.2. Group velocity Dispersion curve of 2-mm thickness Titanium plate structure results for SAFE (a) and for GMM (b).Red line for symmetric wave modes, blue line for asymmetric wave modes.....	50
Figure 5.3. Schematic representation of the phase velocity values corresponding to the four selected frequency values on symmetric and antisymmetric wave modes obtained using the SAFE method.....	51
Figure 5.4. Phase velocity dispersion curve of 3-layered elastic-viscoelastic- elastic obtained from SAFE	55
Figure 5.5. Phase velocity dispersion curve results of 3-layered system from GMM.....	55

Figure 5.6. Attenuation dispersion curve obtained from SAFE method	56
Figure 5.7. Phase velocity dispersion curve of the 3-layered symmetric system with vary thickness ratio of viscoelastic layer embedded between two aluminum plates. Thickness ratio for (a)=0.66.,(b)=0.53., (c)=0.4.,(d)=0.25	58
Figure 5.8. Different viscoelastic layer thickness results on same Phase velocity dispersion curve of three layered system	60

LIST OF TABLES

<u>Table</u>	<u>Page</u>
Table 5.1. Material and acoustic properties of Titanium plate	48
Table5.2. Comparison of the phase velocities of GMM and SAFE methods at four different frequency values for symmetrical zero order (S0) wave mode on a 2 mm thickness Titanium Plate	52
Table5.3. Comparison of the phase velocities of GMM and SAFE methods at four different frequency values for symmetrical zero order (A0) wave mode on a 2 mm thickness Titanium Plate	52
Table5.4. Geometric and Acoustic properties of Elastic-Viscoelastic-Elastic Multilayered structure	53
Table 5.5. Acoustic and material properties of multilayered system.....	57
Table 5.6. Thickness ratios for viscoelastic layer embedded with two elastic plates.....	58

LIST OF SYMBOLS

CHAPTER 3

$A_0, A_1, A_2, \dots, A_n$	Asymmetric wave modes
C_l	Longitudinal wave velocity
C_s	Shear wave velocity
C_g	Group velocity
C_{ph}	Phase velocity
d	thickness
E	Young modulus
f	frequency
i	imaginary unit $i = \sqrt{-1}$
k	wavenumber
$S_0, S_1, S_2, \dots, S_n$	Symmetric wave modes
x_1, x_2, x_3	Cartesian coordinates
u_1, u_2, u_3	Displacements components
w	Angular frequency
$\sigma_{11}, \sigma_{22}, \sigma_{33}$	Stresses components
λ, μ	Lame Parameters
φ	Vectoral potential
ψ	Scaler potential
ν	Poisson's ratio
∇	Vector operator
∇^2	Laplace operator
ρ	Density

CHAPTER 4

A, B	matrices in SAFE equations
B_1, B_2	differential matrices
C	stiffness matrix
d	differential
δH	Hamiltonian
i	imaginary value, $i = \sqrt{-1}$
J	Jacobian matrix
k	wavenumber
k_{real}	real wavenumber
k_{im}	imaginary wavenumber
K_e	Kinetic energy
$k_1^{(e)}, k_2^{(e)}, k_3^{(e)}$	Element stiffness matrices

K_1, K_2, K_3	Global stiffness matrices
$K(k)$	Sum of the global stiffness matrices
$L_x, L_y, L_z,$	matrices in SAFE equations
$m^{(e)}$	Elemental mass matrix
M	Global mass matrix
n_{el}	Number of elements
$N()$	Shape function matrix
$N_1 N_2 N_3$	Component of shape functions
$N_{,y}, N_{,z}$	Derivative of shape functions
$q^{(e)}$	Nodal displacement element
Q	Nodal displacement vector
Q	Eigen vector
Q_R	Right eigen Vector
Q_L	Left eigen vector
t	Time
T	Transformation matrix
u, \dot{u}, \ddot{u}	displacement / velocity / acceleration vector
u_x, u_y, u_z	Displacement components
U_{xi}, U_{yi}, U_{zi}	Displacement components of ith node
V	Volume
W	Potential Energy
x, y, z	Global cartesian coordinates
∂	Partial differential
w	Angular frequency
ρ	Density
Ω_e	Cross-sectional domain representation
σ	Stress vector
$\sigma_{xx}, \sigma_{yy}, \sigma_{zz}, \sigma_{yz}, \sigma_{xz}, \sigma_{xy}$	Components of stress vector
ε	Strain vector
$\varepsilon_{xx}, \varepsilon_{yy}, \varepsilon_{zz}, \varepsilon_{yz}, \varepsilon_{xz}, \varepsilon_{xy}$	Components of strain vector
ξ	Isoparametric element
$(\cdot)^T$	Transpose of matrix
$()^{(e)}$	Elemental

CHAPTER 1

INTRODUCTION

Nowadays, the demand of high quality materials for safer structures in the industry is getting higher. Majority of the structural failures are caused by cracks, corrosion or discontinuities inside material. These problems may be attributed to fatigue, material, poor design, manufacturing process of material or environmental effects. Preventive maintenance is a very crucial for safety practices and enhanced operation of the engineering structures.

There are also some techniques, which may be used to determine hidden defects inside the materials. Two of the most commonly used methods within these techniques are ultrasonic inspection techniques: Non-destructive testing (NDT) and structural health monitoring (SHM). These methods are based on the interference of high-frequency sound waves, which are transduced into the material with the help of the ultrasonic transducer and the discontinuities inside or at surface of the material.

In traditional ultrasonic inspections shear and longitudinal bulk waves are used, in which only a small portion of the structure can be inspected at a single measurement. This technique requires ultrasonic signal source position to be swept on structure in order to cover the whole structure. This process is a very time consuming for inspecting such large structures like pipelines, rails, storage tanks, plates etc. For effective inspection, guided waves offer a very efficient and rapid solution by reducing the inspection efforts and time. The main differences between using traditional bulk waves and guided waves for inspection are illustrated in Figure (1.1) (Rose 2014). The basic difference of guided waves is that inspected structure boundaries is used for as a 'guide' for wave propagation by interacting with the wave signal at given proper angle by using the ultrasonic transducers. These transmitted waves are reflected back and forth from the boundaries of the structure, providing inspection of the whole structure. For those reason, this types of waves is referred as 'guided waves' in acoustic area.

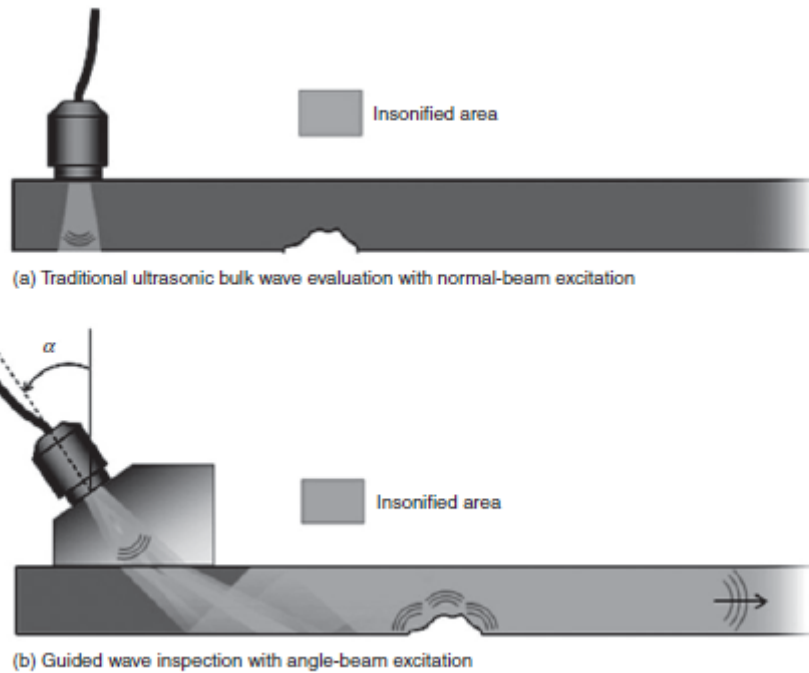


Figure 1.1. Comparison of Bulk wave and Guided wave inspection techniques

(Source: Rose 2014, page-3)

Ultrasonic wave generation usually leads to generation of many wave modes within the structure thickness. This multi-mode wave propagating depends on not only geometric boundaries but also on frequency. The number of wave modes increases with frequency in the inspected area and this relation provides for making available modes selection while detecting the discontinuities or cracks with setting the proper frequency ranges.

The wave propagation problem in multilayered solids are rather complex and the relations can be shown by phase velocity, group velocity, mode shapes and attenuation dispersion curve in the frequency range of interest. These dispersion properties for any SHM or NDT problem need to be extensively analyzed first for proper selection of ultrasonic waves. Then, proper waves can be used to determine the cracks and/or discontinuities, their locations using proper methods and electrical periphery. Usually, reflections are utilized. Understanding of wave attenuation through dispersion curves also help for wave selection and the frequency range. Additionally mode shapes may constitute a strong influence on wave propagation for specific modes, by means of stress, displacement and energy.

implemented in Matlab R-2014b. Matrix based purely analytical method based on the global matrix is used for validation of the results by using the commercial Disperse software.

The thesis consists of six chapters. In the first chapter the practical usage of the guided waves in non-destructive tests and structural health monitoring has been discussed. The differences between guided waves and bulk waves have been presented. Besides, the aim and outline of the thesis are included in this chapter.

The historical backgrounds of the guided waves have been presented from the earlier developments in Chapter 2. Matrix based solution methods with different types of waveguides were presented under the analytical methods section and related studies about approximate methods numerical are also covered in finite element method section. Additionally, hybrid analytical and finite element solution methods are summarized in the last section, which is the main topic of the thesis.

The theoretical derivation of wave equations for unbounded medium has been summarized following Chapter 3. Rayleigh-Lamb wave dispersion is analyzed extensively along with fundamental concepts about guided wave propagation.

The theoretical derivation of the SAFE modelling for guided waves is presented in Chapter 4. The adaptation of the solution method for guided wave problem on a planar structure using 1D line elements in FEM part is summarized with the eigen-value problem from the SAFE formulation. Only Lamb wave modes on a plate model was considered.

Results of the numerical studies with SAFE method were presented in Chapter 5. Generated dispersion curves from the SAFE results are compared with the Disperse software for elastic isotropic plate model first to validate the model considering low order Lamb wave modes. Furthermore, elastic and viscoelastic multi-layered plate configuration was modelled with SAFE method in order to obtain phase velocity dispersion curves and attenuation dispersion curve. Obtained dispersion curves are also compared with the experimentally validated result and modelling issues with loss medium and effects of the viscoelastic layer thickness is also discussed.

In the final Chapter 6, the results of the study are discussed and possible future work is also presented.

CHAPTER 2

LITERATURE SURVEY

For over a century, guided waves problems were investigated by many researchers and engineers in different kinds of areas. In this chapter, the history of ultrasonic guided waves is given under three subtitles. In section 2.1, guided acoustic waves in solid structures will be given based on the studies of guided wave theory in different types of waveguides. In section 2.2, modelling guided acoustic waves in terms of analytical, matrix based methods and finite element modelling are discussed and lastly in 2.3, studies about Semi-Analytical finite element modelling are presented.

2.1 Guided Acoustic Waves in Solids

The earlier studies on surface wave of the structure were introduced by (Rayleigh) in 1885, which was the first theoretical approach of the guided wave phenomena. Then, acoustic waves studied by (Lamb 1917) for isotropic plate in vacuum space. He made derivation of the guided waves characteristic equation and found the dispersion relation between the wave velocity and frequency of the propagating waves in single layer structure. The roots of these characteristic equations show that two different mode which are called symmetric and antisymmetric modes can propagate in this waveguide. After that, guided waves investigated theoretically by adding another solid medium to the system and occurring waves at these interface between solid-solid medium studied by (Stoneley 1924) All these types of waves can propagate both thickness and directional parallel to plane surface of the structure. The other wave type , which is known as shear horizontal (SH) wave was investigated by (Love 1944). In contrast to the plate surface waves, polarization of this type of wave displacement is perpendicular to propagation direction. These types of waves still carry their names (Rayleigh-Lamb, Stoneley and Love waves) today. After these theoretical derivations was made for simple plate structure, the elastic waves propagation in hollow cylinder structure fully studied by (Gazis 1959a) (Gazis 1959b) in these papers. The theory was

set by introducing the 3D elasticity theorem and by applying the Helmholtz decomposition method for decoupling the wave modes. Instead of using longitudinal (L), shear horizontal (SH) and shear vertical (SV) wave modes which are used in planar wave propagation, in cylindrical waves the partial waves are denoted as axial, torsional and flexural wave modes. All modes are investigated under the names of axially symmetric, non-axially symmetric and torsional wave motion. After that, (Viktorov 1967) has presented an extensive research on cylindrical and plate structures. He, firstly, formed characteristic equations and brief explanation on differences between the plate wave and cylindrical wave motion by introducing the angular wavenumber term which is valid for these types of guided waves.

2.2 Modeling Guided Acoustic Waves

The solution of the guided wave equations and analysis of its dispersion relies on modelling acoustic waves by considering boundary conditions and material characteristics. The word “dispersive” means that propagating wave velocity or any other parameter depends on or changes with changing frequency. Most of the studies are related with illustrating these frequency and velocity dependence use dispersion curves, which containing formation about travelling wave behavior in those types of structures.

Considering all these aspects, analytical and numerical models for different type of wave problem has been developed to simulate problems with various boundary and interface condition, composed of layers with different mechanical and acoustic properties.

2.2.1 Analytical Modeling

In the literature, guided wave propagation has been extensively analyzed analytically by using bulk partial waves and Helmholtz decomposition method for isotropic medium. The details about these two methods can be found in (Rose 2014) However, for the multilayered system analytical solution can be studied by superposition of bulk waves, considering individual layers. In this method, interaction

of longitudinal and shear bulk waves at the interfaces, boundaries of the structure and superposition of these waves has to be considered.

There are two different matrix based approaches in the literature. One of them is named as “transfer matrix” method which is proposed by (Thomson 1950) after treated by (Haskell 1953) . In this method, a single layer matrix is employed for representing stress and displacement fields of a single layer, which are created by the wave propagation at both top and bottom surface of single layers. The matrix is multiplied by additional matrices representing all other layers, yielding the transfer matrix. It is reported that these layer-by-layer multiplication yields numerical instabilities for this method when layer thicknesses increase (Lowe 1995) and (Kamal, et. al 2013).

The other method is called as “global matrix method”, (GMM) which is proposed by (Knopoff 1964). This method is based on the assembly of individual layer matrices in a single global matrix, representing the system with considering the traction free condition on surface of the structures and continuity condition at the interfaces between individual layers. Both of these matrix solutions result in an eigenvalue problem, whose roots are gives relation between wavenumber and frequency of propagating waves, from which the dispersion curves can be formed. A good review on both global matrix method and transfer matrix method is given by (Lowe 1995). In this paper, both methods are summarized and root searching algorithm and sweeping techniques for solution in terms of frequency and wavenumber domain is given in detail. In addition to that, implementation of Kelvin-Voigt viscoelastic modelling in matrix based solution formulation is formulated for the waveguides with attenuation.

These matrix methods have been employed in several studies. (Nayfeh and Chimenti 1989) investigated guided wave propagation and generated dispersion curve of multilayered anisotropic structures with giving brief and robust solution by modelling the structure based on using elasticity theory for defining the displacement and stress fields, partial wave methods and matrix based solution methods. In these studies, the solutions are also validated with the experimental results. Their extensive studies on multilayered structure can be found as a reference book for reader published by (Nayfeh 1995). Another good study based on the transfer matrix method is investigated by (Castaings and Hosten 1994). In this paper, delta operator technique is implemented in transfer matrix approach in order to solve numerical instability of this method where the large frequency and thickness product is needed to be effectively handled, while modelling multilayered plates.

Another issue on guided waves inspection is not only modelling wave reflection and refraction from medium interfaces and boundaries but also dealing with viscoelastic waveguides. In a damped medium, travelling waves are attenuated with distance and after a while wave energy might completely vanish because of the energy dissipation. For this reason, modelling mediums with attenuation is crucial, for selecting less attenuated wave modes especially on long range inspection problems, where severe attenuation might cause issues. With considering this issue (Bernard Lowe, & Deschamps, 2001) made good studies on effect of viscoelasticity on dispersion relations of waves. In this studies fluid loaded layer structure model is used and investigated with introducing energy velocity concepts for absorbing and non-absorbing region instead of using group velocity concept. Their results have shown that modelling with complex frequency terms for attenuation is more reasonable for the medium they have investigated. In the case of the medium with losses, experimental results show that energy velocity concept give exactly the same results as group velocity solutions.

Another study with considering attenuation effect due to the viscoelastic coating is made by (Simonetti, 2003). In this study, matrix based methods is used for obtaining dispersion features on multilayered plate system. However the aim of the proposed study is investigated the effect of the viscoelastic coated in hollow cylinders. This plate model is used due to the difficulties of investigating viscoelastic coated by using matrix methods in hollow cylindrical structure. As a result of this study, it is observed that obtained dispersion features on plate like structure can be safely used with thickness to radius ratio up to 0.10. Effects of viscoelastic coating in terms of attenuation due to the material damping on dispersion characteristics are also reported by increase the thickness of the coat in that study.

After that, (Barshinger and Rose 2004) made an analysis on wave dispersion for pipes with viscoelastic coating, which is frequently used against corrosion in pipelines. In this paper, Kelvin-Voigt material damping model is used, where the frequency-dependent Lamé parameters are defined. The solution also yields complex wavenumber values, whose imaginary part corresponds to attenuation values. The multilayered hollow cylindrical structure is modelled with matrix based on GMM. The solution is obtained considering the axisymmetric wave modes only. The dispersion curves are derived with considering attenuation, which are verified with the experimental results and effect of the viscoelastic coated is discussed.

There is commercial software named “Disperse”, which should also be mentioned. It is developed by Imperial College of London NDT groups (Pavlakovic et al. 1997), and currently used as reference in guided wave propagation applications. This software is used for generate dispersion features like phase velocity, group velocity and mode shape of guided waves based on GMM method. It is also capable of working with different waveguides types like cylindrical hollow and plate and their multilayered configurations.

The global matrix method formulation with considering different types of waveguides for guided wave analysis and investigation of wave propagation with cracks are also discussed by (Rose 2014) in detailed. In this reference book, other important guided wave featured like wave scattering and reflection from defects, mode conversions are discussed and attenuation analysis for long range NDT is also covered.

2.2.2 Finite Element Modeling

Guided waves and dispersion analysis of propagating waves have been studied based on analytical and matrix based solution methods for over years. However, when dealing with complex shaped structures like train rail, T shaped beams (C. M. Lee et al., 2006),(Hayashi et al., 2003) or inhomogeneous complex materials (Bartoli, et al., 2006),(Gao 2007), these solution methods are inadequate in order to generate dispersion features or investigate the behavior of the propagating waves with defects. Many researchers and engineers have been resort to finite element methods (FEM) in order to overcome the difficulties associated with complex or irregular shaped waveguides.

In this approach, the main idea is dividing the structure or cross-section into small finite elements (discretization), which are linked to each other through nodal points. Then, set of simpler algebraic equations at each element is used for solving whole domain with using the special interpolation functions, which are set in between each node with considering their boundaries. When dealing with guided wave problems, these algebraic equations are defined by partial differential equations and solved from one element to another element by using numerical approximation.

From the beginning of the 1990s, guided wave simulation and dispersion analysis of wave from defects and selection of wave mode for defect detection have been studied based on traditional FEM approach in different waveguides. Convergence

of the solution and accuracy relations in time domain analysis are studied by (Alleyne and Cawley 1992) and (Moser, Jacobs, and Qu 1999) with using traditional finite element method. Their studies showed that, at least 10 nodes per wavelength should be considered for dispersion analysis and interference of guided waves with defects. Another study about wave scattering from defects is presented by (Demma 2003). In this study, wave reflection from the different types of defects is investigated by shear horizontal (SH) wave modes for plates where propagation direction is perpendicular to wave direction and lying in the horizontal axis and torsional (T) wave modes for circular waveguides. Also, in this study the potential use of such wave modes in non-destructive examinations has been discussed. The wave propagation information revealed by the numerical solutions of the derived wave equations based on analytical expressions is compared with the finite elements.

Another good aspect of using the FE approach is the availability of commercial products such as Comsol, Abaqus etc. These softwares allow modeling complex shaped waveguides with a wide variety of materials easily. Taking into account for its advantages, many studies have been carried out by using these commercial packages. Guided wave propagation in steel plate with discontinuities is discussed by (Juluri 2008) with modelling the structure. In this study, weld quality of storage tanks is investigated by experimentally using longitudinal (L) guided waves. It is also suggested that about the fundamental symmetric wave modes (S0) is more sensitive for long range inspection on welds between two plates. Another good study is done by (Drozdz, 2008), where wave scattering from defects is investigated in elastic media with considering the accuracy of the solution by increased local mesh size.

Although finite element method has many advantages for modelling and solving guided wave problems, these methods can be time consuming when dealing with larger geometries for accurate modal analysis. Another issue with FEM approach is adaptation of the solution with using edge effects for modeling, since in these types of geometric restrictions, wave reflection and refraction might cause problems if not handled properly. In order to overcome these issues, researchers are resorted to improve hybrid finite element models with the aims of reducing computational time and handling the reflection from the edges boundary.

The basic idea of these studies is reducing the dimension of the analysis model. The traditional FEM is analyzed by using three dimensional modelling however, most of the application and guided wave problems can be studied by two dimensional

cases because of constant cross-section shape of waveguide structure. With considering this nature, studies about decreasing computational cost issue are numerous in the literature under the names of Boundary Element Method (BEM) (Cho and Rose 1996) and (Yang and Zhou 1999), Finite Difference Method (FDM) (Balasubramanyam et al.,1996) , Wave Finite Element (WFE) (Manconi and Mace 2007) and etc. All these numerical approaches are done by adopting suitable mathematical manipulations with considering easier way of solving generated differential equations related with modelling guided waves. These approaches have some advantages and disadvantages on modeling different types of guided wave problem. The comparison of these approaches and discussion about capability of analyzing wave propagation can be found in (B. C. Lee and Staszewski 2003) and (Kamal, Gresil, and Giurgiutiu 2013).Another good review of improved methods including analytical matrix based approaches can be found in (Willberg et. al., 2015) with considering time and frequency domain analysis. In those studies, each improved method for making guided wave analysis is discussed with their capability to obtain accurate solutions.

2.3 Semi Analytical Finite Element Modeling

In recent years, the semi-analytical finite element method (SAFE) has been widely used by many researchers in order to solve guided wave problems in many types of structures with different material properties because of the flexibility of the using both FEM and analytical solution of guided waves at the same time. This method is based on analytical solutions of the propagating waves while the finite element discretization domain of the structure is perpendicular to this propagating wave direction is employed. Because of these, it is called as semi-analytical. In general, the solution of the characteristic equation is obtained from the resulting eigenvalue problem. Also, using discretization of 2-D cross sections only render the method as an efficient tool for solving guided wave problems with complex shapes, since more time-consuming 3D discretization is used in traditional FEM approaches. In addition to this, finite element approach uses the material stiffness matrix and virtual work principle makes this approach for the multilayered system,where the material properties is changing at individual layers or combining different materials like composite structures needs to be handled.

2.3.1 SAFE for Modeling of Guided Waves

With considering advantages of this method, studies in the literature are numerous. (Gavrić 1995) as a pioneering study, used two dimensional triangular and quadrilateral shape functions, while discretizing the cross-sectional domain in finite element modelling for noise reduction in rails. In the paper, the solution of resulting eigen-value problem consisting only of evanescent and propagating modes of wave in rails is assumed. Following, this model is adopted and extended for arbitrary cross section structures and studied for all wave modes by (Hayashi, Song, and Rose 2003); theoretical derivation of guided waves is done and its dispersive characteristic are investigated and compared with experimental results. Then, (Bartoli, Marzani, Lanza di Scalea, et al. 2006) extended this method for viscoelastic materials by adopting complex stiffness matrix. As there are different ways of the introducing these damping effect, instead of using Kelvin-Voigt method which is traditionally used in matrix based methods, hysteretic model is used for defining material damping.

Following all these theoretical improvements was, the generalized SAFE approach is employed by many researchers in various waveguides like pipes, rod, plates, and especially complex shaped structures and composites. For the case of the complex shaped waveguides, guided wave analysis proposed by (C. M. Lee 2006). In this study, the SAFE approach was applied to investigate shell defects on rails. Then, according to the experimentally verified results in terms of dispersion, the appropriate wave modes are determined by considering long-range inspection and defect locations. These wave modes and corresponding frequency ranges were then used in the design of special transducers for the purpose of non-destructive evaluations of such defects.

Another important issue with the SAFE theory comes from the resulting wave modes and their distinction from each other, since the eigen solutions includes all modes like propagating, evanescent and non-propagating wave modes. This distinction is very crucial for obtaining dispersion curves and selection of desired wave modes or mode control issue. This problem was studied by (Mu and Rose 2008) on hollow cylinder structure with viscoelastic coatings and solved for guided wave dispersion curves and attenuation characteristics with considering both axisymmetric and flexural wave modes. On the other hand, mode distinction was made by developing an algorithm using the orthogonality relation of each modes result in that study.

Another study is made by (Van Velsor 2009), applied this method for circumferential order multi layered structure with de-coupled circumferential Lamb and shear wave modes with SAFE in multilayered system. In this study, dispersion curves for each decoupled modes are solved with using both GMM and SAFE method for elastic medium. A brief comparison is also made between these two methods and convergence of the solution by SAFE approach is discussed by considering discretized domain mesh size.

Another study is made by (Fan 2010). In this study SAFE approach is used for measurements of the fluid density with using the torsional (Shear) wave modes. The measurements are based on the fact that, shear types waves cannot propagate in inviscid fluids. Measurements with preset dipping distances in dipstick tests yields as inverse guided wave problems, which can be post-processed for the desired material properties of that fluid medium. In addition to that in that study, SAFE approach is also used for analyzing the weldment quality of the plate like structures with considering both longitudinal (L) and shear wave modes (S). The comparison on sensitivity for crack evaluation between these wave modes is also discussed according to the experimental results.

Another issue related with the SAFE method is modelling the whole structure with energy leakage in fluid-embedded systems, which is a particularly important issue for pipeline industries. This phenomenon is studied by (Mazzotti et al. 2013) for cylindrical shaped waveguides. In this study, SAFE formulation is combined with the Boundary Element Method (BEM), by which the surface of the structure is modeled, in order to simulate energy leakage to the system. This new developed SAFE method is used for generating dispersion features of the whole embedded structure and attenuation effect of the load from the fluid are also discussed.

In general case, SAFE method is applied to solve various guided wave problems and another are composites, which are complex multi layered structures. The challenge of doing guided wave analysis on those types of structure comes from the inclusion of viscoelastic layers and anisotropic behavior. SAFE approach was used by (Gao 2007) on composite structure in PhD thesis. In this study, complex stiffness matrix for defining each viscoelastic layers was adopted in SAFE approach and resulting dispersion relations are presented as group and phase velocity curves. On the other hand, the wave structure information of the composite structure illustrated with using GMM. It is reported that, SAFE method is provided faster and accurate results for

dispersion curve generation however, wavestructure information was achieved more accurately by using GMM.

Another study for the case of the composite structure is proposed by (Ahmed, 2011), In this study, dispersion analysis and reflected wave from the edge of the structure and transmission coefficients are analyzed using the SAFE approach, since the addition of such restrictions require additional boundary relations for the solution. Besides these, a new numerical solution procedure for only considering Lamb wave modes from the SAFE approach is proposed.

CHAPTER 3

FUNDAMENTALS OF GUIDED WAVES

3.1 Bulk Waves in Isotropic Media

In order to investigate the propagating wave characteristics it is important to understand the generalized wave equations in unbounded isotropic medium first. In isotropic medium, there are two types of bulk waves that can propagate. One of them is longitudinal waves, in which particle motion is parallel to propagating wave direction. The other type is shear wave, where particle motion is perpendicular to the direction of the propagation. In this section Rayleigh-Lamb wave equations and propagating wave velocities for dispersion relations which are well documented by many books are summarized following (Rose 2014).

3.1.1 Equation of Motion

This approach starts with applying the Newton's second law for an element, is adopted in Cartesian coordinates system (x_1, x_2, x_3) . The equation of motion by omitting force terms for three-dimensional body is given as in Eqn (3.1)

$$\begin{aligned}\frac{\partial \sigma_{11}}{\partial x_1} + \frac{\partial \sigma_{12}}{\partial x_2} + \frac{\partial \sigma_{13}}{\partial x_3} &= \rho \frac{\partial^2 u_1}{\partial t^2} \\ \frac{\partial \sigma_{21}}{\partial x_1} + \frac{\partial \sigma_{22}}{\partial x_2} + \frac{\partial \sigma_{23}}{\partial x_3} &= \rho \frac{\partial^2 u_2}{\partial t^2} \\ \frac{\partial \sigma_{31}}{\partial x_1} + \frac{\partial \sigma_{32}}{\partial x_2} + \frac{\partial \sigma_{33}}{\partial x_3} &= \rho \frac{\partial^2 u_3}{\partial t^2}\end{aligned}\tag{3.1}$$

,where u_1, u_2 and u_3 are the displacements, ρ is the density of three dimensional element, t is the time and $\sigma_{11}, \sigma_{22}, \sigma_{33}$ etc. representing the stress field on the faces of this element. These fundamental stress terms in equation (3.1), can be expressed in terms of strain-stress and strain-displacement relations.

The stress-strain relation can be written in tensor notation with considering isotropic medium can be written as;

$$\sigma_{ij} = \lambda \varepsilon_{kk} \delta_{ij} + 2\mu \varepsilon_{ij} \quad (3.2)$$

where μ and λ are the Lamé parameters for isotropic material. δ_{ij} represents the Kronecker delta operator with subscript i and j numbering with (1, 2 and 3) corresponding to unit directions. ε_{kk} represents total change in volume (dilatation) of this element, where can be written as;

$$\varepsilon_{ij} = \frac{1}{2}(u_{i,j} + u_{j,i}) \quad (3.3)$$

$$\delta_{ij} = \begin{cases} 1 & i = j \\ 0 & i \neq j \end{cases}, \quad \varepsilon_{kk} = \varepsilon_{11} + \varepsilon_{22} + \varepsilon_{33} \quad (3.4)$$

Substituting Eqn (3.3) and Eqn (3.4) into Eqn (3.2) Stress fields yields;

$$\begin{aligned} \sigma_{11} &= \lambda \varepsilon_{kk} \delta_{ij} + 2\mu \varepsilon_{11}, & \sigma_{22} &= \lambda \varepsilon_{kk} \delta_{ij} + 2\mu \varepsilon_{ij}, \\ \sigma_{33} &= \lambda \varepsilon_{kk} \delta_{ij} + 2\mu \varepsilon_{33} \\ \sigma_{12} &= 2\mu \varepsilon_{12}, & \sigma_{23} &= 2\mu \varepsilon_{23}, & \sigma_{13} &= 2\mu \varepsilon_{13} \end{aligned} \quad (3.5)$$

The strain-displacement relation can be written as;

$$\varepsilon_{ij} = \frac{1}{2}(u_{i,j} + u_{j,i}), \quad i, j = 1, 2, 3 \quad (3.6)$$

In explicit formula with introducing the i, j to the strain displacement relation yields;

$$\begin{aligned} \varepsilon_{11} &= \frac{\partial u_1}{\partial x_1}, & \varepsilon_{22} &= \frac{\partial u_2}{\partial x_2}, & \varepsilon_{33} &= \frac{\partial u_3}{\partial x_3} \\ \varepsilon_{12} &= \frac{\partial u_1}{\partial x_2} + \frac{\partial u_2}{\partial x_1}, & \varepsilon_{23} &= \frac{\partial u_2}{\partial x_3} + \frac{\partial u_3}{\partial x_2}, & \varepsilon_{13} &= \frac{\partial u_1}{\partial x_3} + \frac{\partial u_3}{\partial x_1} \end{aligned} \quad (3.7)$$

Substituting the strain- displacement relation in Eqn (3.6) and stress-displacement relation in Eqn (3.5) into the equation of motion Eqn (3.1) and rearranging terms,

generalized displacement equation of motion is also known as ‘Navier’s equation of motion’ can be obtained as;

$$\begin{aligned}
(\lambda + \mu) \frac{\partial}{\partial x_1} \left(\frac{\partial u_1}{\partial x_1} + \frac{\partial u_2}{\partial x_2} + \frac{\partial u_3}{\partial x_3} \right) + \mu \nabla^2 u_1 &= \rho \frac{\partial^2 u_1}{\partial t^2} \\
(\lambda + \mu) \frac{\partial}{\partial x_2} \left(\frac{\partial u_1}{\partial x_1} + \frac{\partial u_2}{\partial x_2} + \frac{\partial u_3}{\partial x_3} \right) + \mu \nabla^2 u_2 &= \rho \frac{\partial^2 u_2}{\partial t^2} \\
(\lambda + \mu) \frac{\partial}{\partial x_3} \left(\frac{\partial u_1}{\partial x_1} + \frac{\partial u_2}{\partial x_2} + \frac{\partial u_3}{\partial x_3} \right) + \mu \nabla^2 u_3 &= \rho \frac{\partial^2 u_3}{\partial t^2}
\end{aligned} \tag{3.8}$$

This displacement equation of motion in Eqn (3.8) can also be expressed in vector form in Eqn (3.9);

$$(\lambda + \mu) \nabla \nabla \cdot \mathbf{u} + \mu \nabla^2 \mathbf{u} = \rho \frac{\partial^2 \mathbf{u}}{\partial t^2} \tag{3.9}$$

In this expression, ∇ represents the vector operator $(\hat{x}_1 \frac{\partial}{\partial x_1}, \hat{x}_2 \frac{\partial}{\partial x_2}, \hat{x}_3 \frac{\partial}{\partial x_3})$ and ∇^2 represents the Laplace operator $(\frac{\partial^2}{\partial x_1^2} + \frac{\partial^2}{\partial x_2^2} + \frac{\partial^2}{\partial x_3^2})$.

The equation of motion and the relationship between stress and strain in an isotropic elastic medium are used to derive the elastic wave equation. The total system of equation just obtained in equation (3.9). This equation has three displacement fields which are introduced with \mathbf{u} . These displacement fields are uniform and constant in all directions due to isotropy of medium however, it is difficult to solve directly. For this reason the equation can be uncoupled by introducing the Helmholtz Decomposition method.

3.1.2 Helmholtz Decomposition method

In order to apply this method, displacement vector \mathbf{u} in Eqn (3.9) can be expressed in terms of derivatives of scalar and vector potentials by using Eqn (3.10) to define dilatational and rotational displacements in medium respectively. (See also (Achenbach 1975) section-6).

$$\mathbf{u} = \nabla\varphi + \nabla \times \psi, \quad \nabla \cdot \psi = 0 \quad (3.10)$$

In this representation, displacement fields consist of the sum of the gradient of the scalar potential φ and curl of the vector potential ψ which should satisfy the general expression. By applying the method of potential Eqn (3.10) in vector form of equation of motion in Eqn (3.9) yields as follow in Eqn (3.11);

$$\begin{aligned} & (\lambda + \mu)\nabla(\nabla \cdot (\nabla\varphi + \nabla \times \psi)) + \mu\nabla^2(\nabla\varphi + \nabla \times \psi) \\ & = \rho \frac{\partial^2}{\partial t^2} (\nabla\varphi + \nabla \times \psi) \end{aligned} \quad (3.11)$$

where; $(\nabla \cdot (\nabla \times \psi) = 0)$ and $(\nabla \cdot \nabla\varphi = 0)$ (3.12)

Applying vector identities and rearrangement by using (3.12), this equation can be separated two different wave fields;

$$\nabla \left[(\lambda + \mu)\nabla^2\varphi - \rho \frac{\partial^2\varphi}{\partial t^2} \right] + \nabla \times \left[\mu\nabla^2\psi - \rho \frac{\partial^2\psi}{\partial t^2} \right] = 0 \quad (3.13)$$

This expression can only be solved if these uncoupled terms within the square brackets in Eqn (3.13) are both equal to zero. So, these equations can be shown following uncoupled wave equations;

$$\nabla^2\varphi = \frac{1}{C_l^2} \frac{\partial^2\varphi}{\partial t^2} \quad (3.14)$$

$$\nabla^2\psi = \frac{1}{C_s^2} \frac{\partial^2\psi}{\partial t^2} \quad (3.15)$$

As a consequence, equation of motion (3.9) is decomposed in terms of two uncoupled wave equations (3.14) and (3.15) with respect to particle motion types. In the first expression, C_l represents the longitudinal (pressure) P-wave. This wave motion leads to change of volume of the medium. C_s represents the shear (transverse) S-wave in which, wave motion leads to rotation motion without causing any changes in volume.

3.1.3 Bulk Longitudinal and Shear wave velocities

This generalized uncoupled wave equation is solved by substituting harmonic wave assumption for both expressions as in equation (3.16)

$$\begin{aligned}\varphi &= A(L)e^{i(k.x-\omega t)}, \\ \psi &= A(S)e^{i(k.x-\omega t)}\end{aligned}\quad (3.16)$$

These general exponential terms is used for describing harmonic wave behavior in medium with changing time. In these expression, x denotes as three displacement directions (as a vector), $A(L)$, $A(S)$ are representing the longitudinal and shear wave amplitudes, k is the wavenumber vector and $w = 2\pi f$ is the angular frequency of the propagating waves. The wavenumber vector is used for describing propagating wave velocity and wavelength with the use of these relations;

$$Wavelength = \frac{2\pi}{k} \quad \text{and} \quad Phase\ Velocity(c) = \frac{w}{k}$$

Substituting these harmonic wave expressions in equation (3.16) into the uncoupled wave equations (3.14 and 3.15) is giving form of bulk longitudinal C_l and shear wave C_s velocities in terms of mechanical properties (Lame) of material;

$$C_l^2 = \frac{\lambda+2\mu}{\rho}, \quad C_s^2 = \frac{\mu}{\rho} \quad (3.17)$$

These solutions show that there are two different types of waves can propagate in isotropic unbounded medium with the constant velocity which is determined by directly using mechanical properties of medium. These Lamé parameters μ and λ can be given as in equation (3.18);

$$\mu = \frac{E}{2(1+\nu)} \quad \text{and} \quad \lambda = \frac{E\nu}{(1+\nu)(1-2\nu)} \quad (3.18)$$

where, E and ν are representing Young modulus and Poisson's ratio of the material respectively.

3.2 Guided Wave in Isotropic Media

Previous section we considered bulk wave propagation in unbounded isotropic medium. On the other hand, in the bounded medium wave propagation highly depends on structure boundaries, from which continuous reflection and refraction in between parallel surfaces occur. Wave propagation in bounded layers can be modelled by using bulk shear and longitudinal waves considering the boundary conditions at the plate surface are also considered.

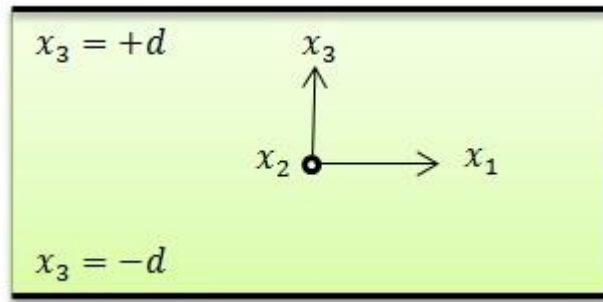


Figure 3.1. Guided wave plate model for isotropic elastic bounded medium with the directions (x_1, x_2, x_3)

Let's consider the wave propagation is invariant in direction x_2 by assuming plain strain condition for simplicity (2D case). The geometry of problem can be illustrated in Figure (3.1). This problem consists of plane wave motion which means that wave propagation only occurs in infinite medium within parallel surfaces. This means that there is no displacement in x_2 direction and at the surface of plate $x_3 = -d$ and $x_3 = +d$ are assumed as a free to traction. By using equation in (3.14) and (3.15) as demonstrated previously decoupled wave equation which satisfying these two dimensional wave equations can be written as ;

$$\frac{\partial^2 \varphi}{\partial x_1^2} + \frac{\partial^2 \varphi}{\partial x_3^2} = \frac{1}{C_l^2} \frac{\partial^2 \varphi}{\partial t^2} \quad (3.19)$$

$$\frac{\partial^2 \psi}{\partial x_1^2} + \frac{\partial^2 \psi}{\partial x_3^2} = \frac{1}{C_s^2} \frac{\partial^2 \psi}{\partial t^2} \quad (3.20)$$

As a result of the plain strain assumption, stress and displacement fields from Hooke's Law can be expressed by using potentials as in equation (3.21).

$$\begin{aligned}
u_1 &= \left[\frac{\partial \varphi}{\partial x_1} + \frac{\partial \psi}{\partial x_3} \right] \\
u_2 &= 0 \\
u_3 &= \left[\frac{\partial \psi}{\partial x_1} + \frac{\partial \varphi}{\partial x_3} \right] \\
\sigma_{31} &= \mu \left(\frac{\partial u_3}{\partial x_1} + \frac{\partial u_1}{\partial x_3} \right) = \mu \left(\frac{2 * \partial^2 \varphi}{\partial x_3 \partial x_1} - \frac{\partial^2 \psi}{\partial x_1^2} + \frac{\partial^2 \psi}{\partial x_3^2} \right) \\
\sigma_{33} &= \lambda \left(\frac{\partial^2 \varphi}{\partial x_3^2} + \frac{\partial^2 \varphi}{\partial x_3^2} \right) + 2\mu \left(\frac{\partial^2 \varphi}{\partial x_3^2} - \frac{\partial^2 \psi}{\partial x_1 \partial x_3} \right)
\end{aligned} \tag{3.21}$$

The exact solution of these equations can be found by assuming the harmonic wave $e^{i(kx_1 - \omega t)}$ for each potential. Where k and ω are terms that represent wave number and angular frequency respectively, $i = \sqrt{-1}$ and x_1 is representing direction of wave propagation. These harmonic wave assumptions can be given as in equation (3.22) and (3.23)

$$\varphi = \varphi(x_3) e^{i(kx_1 - \omega t)} \tag{3.22}$$

$$\psi = \psi(x_3) e^{i(kx_1 - \omega t)} \tag{3.23}$$

In these solution, $\varphi(x_3)$ and $\psi(x_3)$ represent standing waves in x_3 direction while propagating wave direction is defined by x_1 . This means that wave propagation direction has constant displacement distribution on transverse direction x_3 . Substituting these assuming harmonic wave solution into the decoupled wave potentials in equations (3.19) and (3.20) gives the general solution of wave propagation for that bounded layer as in equation (3.24) and (3.25);

$$\frac{\partial^2 \varphi(x_3)}{\partial x_3^2} + \left(\frac{\omega^2}{C_l^2} - k^2 \right) \varphi(x_3) = 0 \tag{3.24}$$

$$\frac{\partial^2 \psi(x_3)}{\partial x_3^2} + \left(\frac{\omega^2}{C_s^2} - k^2 \right) \psi(x_3) = 0 \tag{3.25}$$

Then, solutions of these obtained ordinary differential equations come up with these resulting equations;

$$\varphi = \varphi(x_3) = A_1 \sin(px_3) + A_2 \cos(px_3) \quad (3.26)$$

$$\psi = \psi(x_3) = B_1 \sin(qx_3) + B_2 \cos(qx_3) \quad (3.27)$$

where;

$$p^2 = \frac{w^2}{c_t^2} - k^2 \quad \text{and} \quad q^2 = \frac{w^2}{c_s^2} - k^2 \quad (3.28)$$

A_1, B_1, A_2 and B_2 are the scalar quantities representing wave amplitudes. The indices 1 and 2 in amplitudes also represent propagating wave modes in and out of plane directions with respect to mid plane of the structure. Introducing these harmonic solutions in equations (3.26) and (3.27) into the displacements and stress fields by using equations (3.21) which is derived under the plain strain assumption yields;

$$\begin{aligned} u_1 &= \left[ik\varphi + \frac{\partial\psi}{\partial x_3} \right] \\ u_3 &= \left[ik\psi + \frac{\partial\varphi}{\partial x_3} \right] \\ \sigma_{31} &= \mu \left(k^2\psi + \frac{\partial^2\psi}{\partial x_3^2} + 2ik \frac{\partial\varphi}{\partial x_3} \right) \\ \sigma_{33} &= \lambda \left(-k^2\varphi + \frac{\partial^2\varphi}{\partial x_3^2} \right) + 2\mu \left(k^2\psi + \frac{\partial^2\varphi}{\partial x_3^2} - ik \frac{\partial\psi}{\partial x_3} \right) \end{aligned} \quad (3.29)$$

In order to understand the wave propagation we should go one step further by using the fact that, equations in Eqn (3.26) and Eqn (3.27) consists of cosine and sine functions with the dependence on x_3 direction. These functions are odd and even respectively. As a result, displacement and stress fields can be separated into two wave modes: symmetric and antisymmetric wave modes with respect to mid plane of medium. They can be presented in term of displacement and stress fields by introducing the generalized harmonic potential solutions in equation (3.26) and (3.27) into the equation (3.29). Then the resulting equations can be given as a two set of solutions in terms of displacement and stress field as in equation (3.30) and (3.31);

Symmetric modes;

$$\begin{aligned}
\varphi &= A_2 \cos(px_3) \\
\psi &= B_1 \sin(qx_3) \\
u_1 &= -ikA_2 \cos(px_3) + qB_1 \cos(qx_3) \\
u_3 &= -ikB_1 \sin(qx_3) - pA_2 \sin(px_3) \\
\sigma_{31} &= \mu(-2ikpA_2 \sin(px_3) + (k^2 - q^2)B_1 \sin(qx_3)) \\
\sigma_{33} &= \lambda(k^2 + p^2)A_2 \cos(px_3) - 2\mu(p^2 A_2 \cos(px_3) \\
&\quad + ikqB_1 \cos(qx_3))
\end{aligned} \tag{3.30}$$

Antisymmetric modes;

$$\begin{aligned}
\varphi &= A_1 \sin(px_3) \\
\psi &= B_2 \cos(qx_3) \\
u_1 &= +ikA_1 \sin(px_3) - qB_2 \sin(qx_3) \\
u_3 &= -ikB_2 \cos(qx_3) + pA_1 \cos(px_3) \\
\sigma_{31} &= \mu(2ikpA_1 \cos(px_3) - (k^2 - q^2)B_2 \cos(qx_3)) \\
\sigma_{33} &= -\lambda(k^2 + p^2)A_1 \sin(px_3) - 2\mu(p^2 A_1 \sin(px_3) \\
&\quad - ikqB_2 \sin(qx_3))
\end{aligned} \tag{3.31}$$

It is also worth to noting that, this generalized symmetric and antisymmetric wave motion is an essential case for isotropic structure with respect to mid plane of plate. These wave motions are illustrated in Figure (3.2).

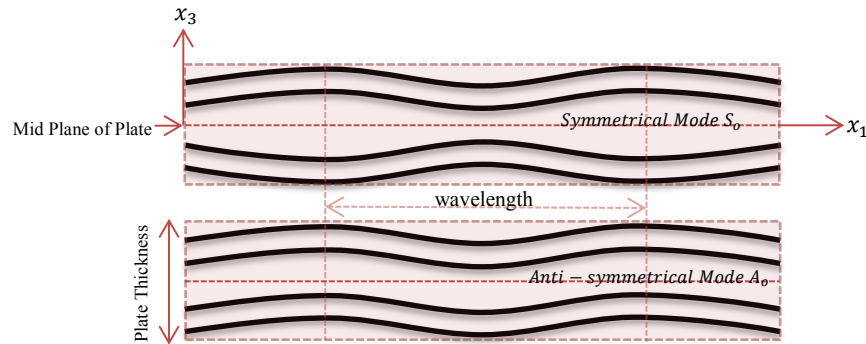


Figure 3.2. Symmetric and Antisymmetric wave modes representation on plate

However, there are also unknown variables which are used for defining the wave amplitudes, A_1 , B_1 , A_2 and B_2 . These quantities can be evaluated by applying boundary

conditions as proposed at the beginning of the modelling. These boundary conditions state that stresses at the lower and upper surface of the structure is zero;

$$\sigma_{31} = \sigma_{33} = 0 \quad \text{at } x_3 = \pm d \quad (3.32)$$

Considering of two wave modes solutions, displacements and stresses given in equation (3.30) and (3.31), then applying these boundary conditions into the generalized wave motions yields the homogenous equations which have constant wave amplitudes A_1, A_2, B_1 and B_2 . After applying the boundary conditions, generated homogenous equations in order to non-trivial solution coefficient of equations can be omitted since they turn out as constant variables. Then, these homogenous equations can be rewritten as in equations (3.33) and (3.34), leading to dispersion characteristics of the Lamb waves;

$$\frac{(k^2 - q^2)\sin(qd)}{2ikp(\sin(pd))} = -\frac{2\mu ikq(\cos(qd))}{(\lambda k^2 + \lambda p^2 + 2\mu p^2)\cos(pd)} \quad (3.33)$$

$$-\frac{(k^2 - q^2)\cos(qd)}{2ikp(\sin(pd))} = \frac{2\mu ikq(\sin(qd))}{(\lambda k^2 + \lambda p^2 + 2\mu p^2)\sin(pd)} \quad (3.34)$$

These obtained equations can be simplified by using the bulk wave velocity definitions in equation (3.17). Substitution of these definitions into the equation (3.33) and (3.34) gives more compact form of the equations for symmetric and antisymmetric wave modes.

$$\frac{\tan(qd)}{\tan(pd)} = -\frac{4k^2pq}{(q^2 - k^2)^2} \quad \text{for symmetric modes} \quad (3.35)$$

$$\frac{\tan(qd)}{\tan(pd)} = -\frac{(q^2 - k^2)^2}{4k^2pq} \quad \text{for antisymmetric modes} \quad (3.36)$$

Where, p and q are given in the form of ;

$$p^2 = \frac{w^2}{C_l^2} - k^2 \quad (3.37)$$

$$q^2 = \frac{w^2}{C_s^2} - k^2 \quad (3.38)$$

As a result, these derived equations are known as ‘‘Rayleigh-Lamb wave dispersion equations’’ in the form of symmetric and antisymmetric wave modes. These equations can be solved numerically for the relation between frequency (ω) and wavenumber (k) of propagating wave modes, which satisfy the boundary conditions of plate structure.

There are also some different types of waves that can exist on given structure configurations which are consisted of different material and interfaces with vary boundaries. For the simplest case of the wave that propagates on the surface of the solid medium with semi-infinite free surface, wave propagation and theoretical derivation is first made by (Rayleigh 1885). The observation from this study is that, the particular motion by the wave propagation are coupled two types of waves which are longitudinal and shear waves in that solid medium. While this coupled wave propagates in the medium, the amplitude of wave are decaying with distance in perpendicular direction from the surface of the structure by assuming the infinite medium. The physical meaning of this behavior is that, the energy of wave are concentrated on the surface of the structure since being in a vacuum space there is no energy leakage from the solid medium. Besides this, this surface wave moves with constant wave speed with frequency on the surface. This is the main differences between guided waves and surface waves; in general, for the case of the surface waves the velocity remains constant with frequency which means non-dispersive. These types of waves are the special case of the wave propagates in between solid-vacuum interface and it is referred as Rayleigh surface wave.

This comprehensive study also leads to investigate the other types of the interface waves with adding the new medium to the system such as; solid-solid medium as (Stoneley 1924) wave and solid-fluid medium as Scholte waves (1942) which are named after by their founder. For instance, the case for the solid-fluid interface, the wave propagation can be existed in fluid medium in contrast to the vacuum space which means that some of the propagating wave energy leakage is occurred between the solid medium and fluid medium when compared with the vacuum space as in the Rayleigh surface wave. As a resulting of this, the surface of the solid medium are not considered as stress free and the boundary conditions at the interfaces between solid and fluid medium are changed. Then, the behavior of these interface waves can be investigated with considering boundary conditions and the acoustic properties of these two medium.

Another wave types for the isotropic elastic solid medium by adding an another vacuum space is studied by (Lamb 1917). These types of waves are refered as special case of guided wave since the wave propagation is guided by the surface of the structures which means there is no energy leakage due to the being in a vacuum space. In this case, in contrast to the assuming infinite solid medium, the thickness of the plate was assumed very small when compare with the wavelength of the propagating waves. As a resulting of this, the multiple reflections of the propagating longitudinal and shear wave between these two paralel surfaces of the plate was occurs. These types of waves in plates are refered as a Lamb waves. In true sense, these waves are very dispersive which means that the propagating wave velocity are changing with frequency and thickness of the plate and multiple reflection of the wave resulted in the many wave modes propagation within the plate. For those reason, wave propagation on plate like structures are also refered as a guided Lamb waves in the acoustic area. Then, this dispersive behavior of the guided Lamb wave in plate like structures can be illustrated by obtaining the dispersion features like phase velocity, group velocity dispersion curves and modes shapes.

Rayleigh-Lamb wave equations are derived theoretically by using isotropic elastic plate structure in vacuum space. Propagating symmetric (S) and antisymmetric (A) wave modes are also derived for understanding of propagating wave behavior. On the other hand, these obtained equations are transcendental which means that solution of these equations can be done by numerically. As can be seen from the generalized equation (3.35) and equation (3.36) the coefficients p and q depends on the angular frequency ($\omega = 2\pi f$), wavenumber (k), shear and longitudinal bulk wave velocities which are determined directly from mechanical properties of materials and thickness (d) of the medium. This dependence is evidence of the dispersive nature of guided Lamb waves since; at each frequency only the specific combination of them is satisfying those equations.

The basic concept of illustrating these relations is plotting wavenumber-frequency solution of generalized wave equations as dispersion curve in Figure (3.3). As an example, 1-mm thickness Aluminum plate which having longitudinal ($C_1 = 6200 \text{ m/s}$) and shear ($C_s = 3200 \text{ m/s}$) wave velocities and density of medium as ($\rho = 2770 \text{ kg/m}^3$) is used.

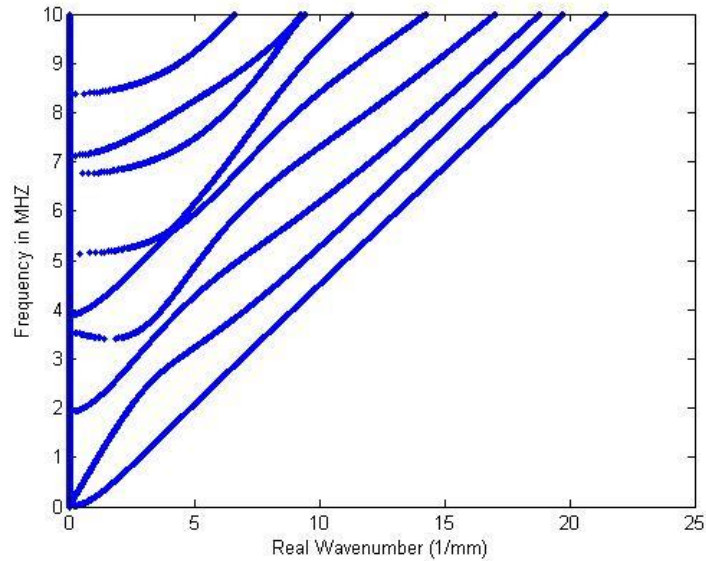


Figure 3.3. Frequency-Wavenumber dispersion curve of 1-mm thickness Aluminum plate

As you can see from the Figure (3.3), for a given frequency there exist a many propagating wave modes which are being reflected from the bounded surface. At each frequency, there are at least two different wavenumber solutions corresponding to fundamental symmetric (S_0) and antisymmetric (A_0) wave modes and increasing frequency thickness product also leads to higher order symmetric ($S_1, S_2, S_3 \dots S_n$) and antisymmetric ($A_1, A_2, A_3 \dots A_n$) Lamb wave modes.

3.2.1 Phase and Group Velocity

Another concept of guided wave propagation is coming from that these waves are travelling as a group in bounded structures, which lead to two velocity concepts. These are group velocity and phase velocity concepts, which are discussed in this section.

Group velocity can be defined as the velocity of the whole traveling wave packets, as they affect each others propagation characteristics. On the other hand, phase velocity is defined as speed of an individual wave crest at that frequency in this wave packet. This relation is illustrated in Figure (3.4)

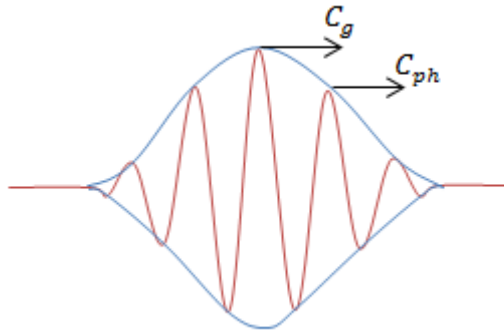


Figure 3.4. Group velocity and Phase velocity representation

Both velocities can be calculated for any propagating wave and also for Lamb waves in plates. These velocities are highly dispersive and changeable for each wave modes in nature. These features are usually expressed in phase velocity and group velocity dispersion curves.

The dispersion curves gives information about each travelling wave velocity (or number) with respect to frequency. These relations can be determined from calculating wave velocity at each frequency by using this expression;

$$C_{ph} = \frac{w}{k} \quad (3.39)$$

Recall from the previous section, by adopting this expression into the Rayleigh-Lamb wave solution gives the phase velocities of each mode against the frequency range. In order to show this, 1-mm thickness Aluminum plate is used for generate phase velocity dispersion curve again. Result is given in Figure (3.5)

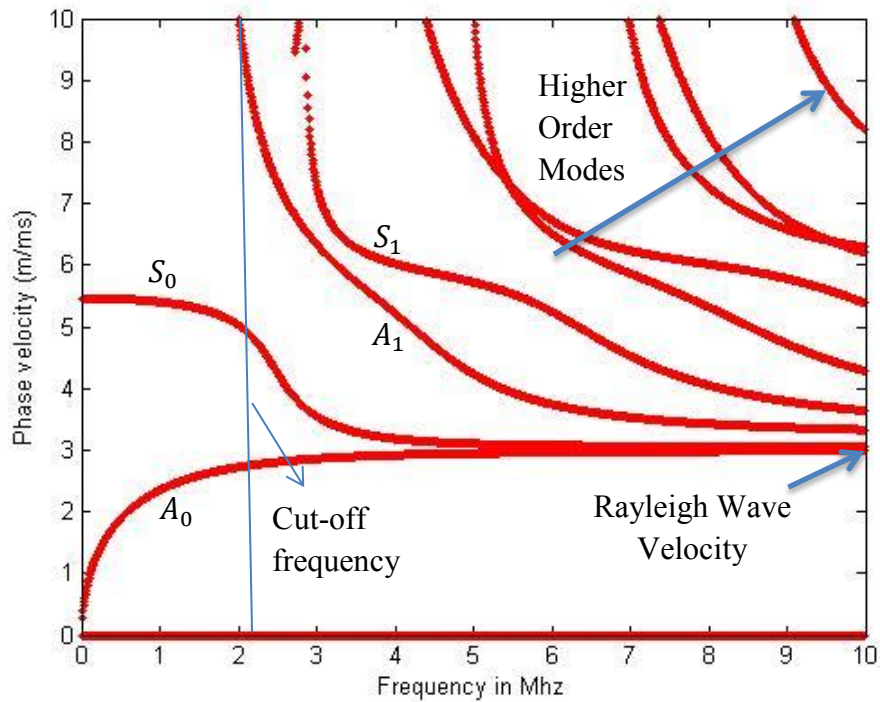


Figure 3.5. Phase velocity dispersion curve of 1-mm Aluminum Plate model

As you can see from the Figure (3.5), symmetric and antisymmetric wave modes and their velocities changes with changing frequency. Four lowest Lamb wave modes are shown and assigned with (A_0, S_0, A_1, S_1) two of them fundamental modes A_0, S_0 two of them first order modes A_1, S_1 . The fundamental wave modes (0) can be present in the whole frequency range. However, higher order modes beginning from the first order can propagate only after a specific frequency value. This frequency is known as cut-off frequency. For instance, below the cut-off frequency only two fundamental modes can travel in plate. On the other hand, when frequency is increased about 4-MHz four different modes can be travel in that medium.

Another important aspect of Lamb waves is that, when frequency is increased all the modes converge to Rayleigh wave velocity because of the superposition of travelling waves in plate. The physical meaning of this is that a displacement field created by wave motion is concentrate at the surface of the plate. For this reason, Rayleigh waves are also referred as a surface waves.

Group velocity concept is another dispersive feature of guided waves. As mentioned before, travelling waves can be propagate as a group wave packets which can consist of waves with different frequencies and varying travelling wave speeds. As a result, the speed of the whole wave packets become as group wave speed. Group

velocity is also referred as a signal velocity of travelling waves. This relation can be defined by differentiation of frequency with respect to wavenumber.

$$C_g = \frac{\partial w}{\partial k} \quad (3.40)$$

This relation can also be derived by using phase velocity expression by using equation in (3.38);

$$k = \frac{w}{C_{ph}} \quad (3.41)$$

Substituting generated wavenumber expression in equation (3.40) into the group velocity relation (3.39) yields;

$$\begin{aligned} C_g &= dw \left[d \left(\frac{w}{C_{ph}} \right) \right]^{-1} = dw \left[\frac{dw}{C_p} - w \left(\frac{dC_{ph}}{C_{ph}^2} \right) \right]^{-1} \\ &= C_{ph}^2 \left[C_{ph} - w \left(\frac{dC_{ph}}{dw} \right) \right]^{-1} \end{aligned} \quad (3.42)$$

Then, substitution of frequency expression ($w = 2\pi f$) into the differentiation in equation (3.41) yields the resulting expression;

$$C_g = C_{ph}^2 \left[C_{ph} - (fd) \left(\frac{dC_{ph}}{d(fd)} \right) \right]^{-1} \quad (3.43)$$

These generalized group velocity equations states that when wave travelling in the non-dispersive region, which means phase velocity is not changing with frequency; group velocity is equal to phase velocity. On the other hand, when propagating wave velocity increases with frequency, group velocity gets larger than the phase velocity. These features are used for structural health monitoring applications extensively.

Another good knowledge is that wave signals are carrying energy in true sense. The group velocity dispersion curve gives knowledges about the propagating wave modes energy in different frequency range in the same manner. For those reasons, group velocity dispersion curve are also referred as energy curve. The resulting group velocity dispersion curve is given in Figure (3.6). The material properties of plate is given as longitudinal ($C_l = 6200 \text{ m/s}$) and shear ($C_s = 3200 \text{ m/s}$) wave velocities and density ($\rho = 2770 \text{ kg/m}^3$) respectively.

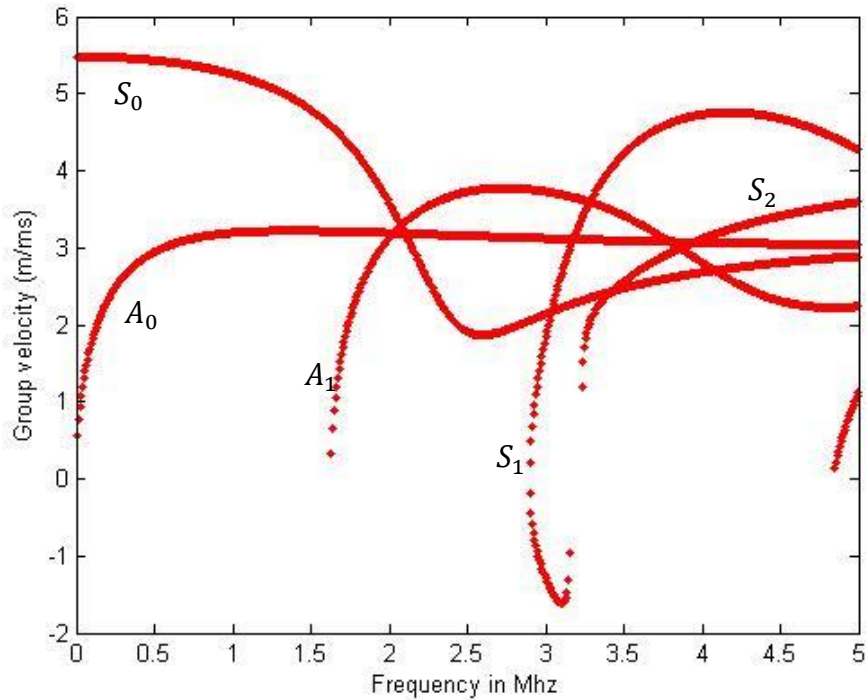


Figure 3.6. Group velocity dispersion curve of 1-mm Aluminum plate

As you can see from Figure (3.6), 5 lowest Lamb wave modes and corresponding group velocity dispersion curve are shown. Up to about 1.6 Mhz frequency-thickness product there are only two fundamental modes which can propagate and easy to distinct each other from group velocity values. These are fundamental symmetric S_0 and antisymmetric A_0 modes.

While making an analysis on a structure selecting the application signals up to 1.6 MHz yields two modes propagation in the medium. Among them, S_0 mode is faster than A_0 modes up to that range. As a result, as mentioned before response signal from any crack or discontinuities in that structure can be determined by using S_0 modes (Juluri 2008) because of earlier wave signals are corresponded to that. In general case, these identification and S_0 is very crucial and extensively used in application area and finding the discontinuities location.

3.2.2 Modes and Mode Shapes

The mode shapes of the propagating waves are also essential tools to understand the nature of these waves. They are also known as wave structures. They show

information about the displacement, stress, and energy magnitudes created by propagating wave along the thickness for different wave modes and frequencies. As a result, this information is used for choosing variety range of modes for analyzing different kinds of discontinuities and hidden defects locations inside the medium. In order to better explain on this issue, desired wave structures on symmetric S_0 and asymmetric A_0 wave modes at different frequency are illustrated in Figure (3.7) with considering various (fd) products on aluminum plates. This frequency-thickness products (fd) representation for wave structures is coming from the fact, the obtained Rayleigh-Lamb wave equation in Eqn (3.35) and (3.36) is a function of this multiplication. These dependence can be used on representing dispersion relations.

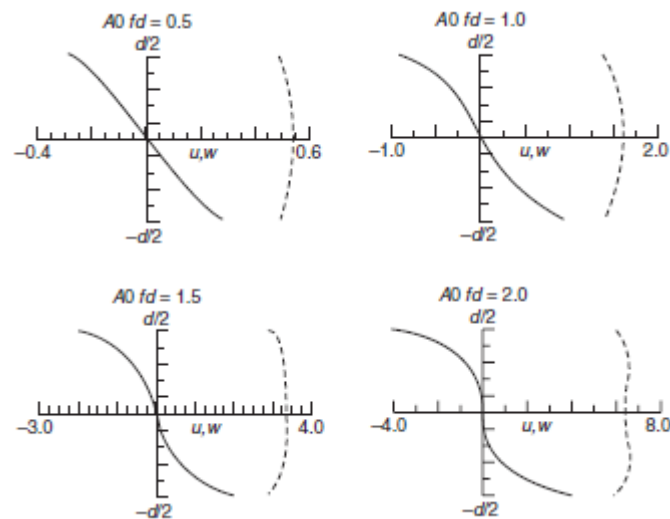


Figure 3.7. Wave structure for different points on S_0 and A_0 wave mode of Aluminum plates with in plane displacement (u , solid line) and out-of plane displacement (w , dashed line) **(cont. on next page)**

(Source: Rose 2014 / page 92-93)

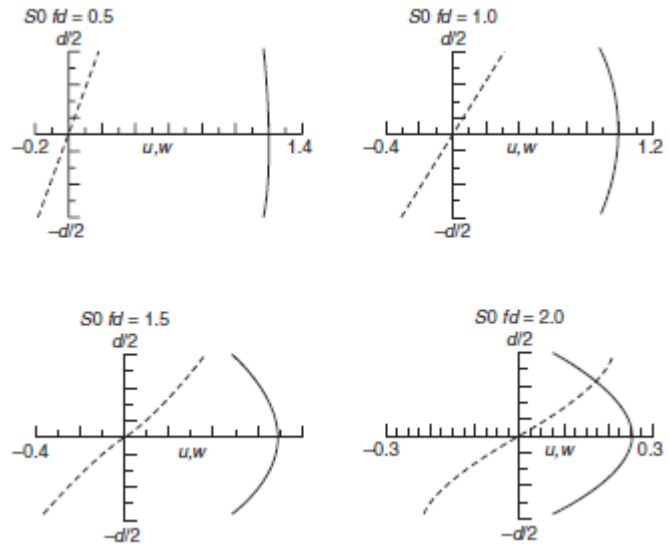


Figure 3.8. (cont.)

As can be seen from the Figure (3.7), at each frequency thickness products (fd), different wave structure information can be obtained along the plate thickness on different modes. These wave structures give the information about which modes to choose and which have higher sensitivity on specific defect locations. For instance, the in plane displacement (u) with increasing (fd) products on A_0 modes keeps the displacement influence on along the thickness direction especially mid plane of the plates, however, in the S_0 modes, increasing (fd) yields more in plane displacement distribution. These examinations demonstrate the ability of usage wave structures on focusing specific defects with considering more sensitive modes evaluations.

CHAPTER 4

SEMI-ANALYTICAL FINITE ELEMENT METHOD

In the previous chapter, guided wave propagation in isotropic plate structure is presented with considering only specific combinations of the frequency, wavenumber and material properties of that medium. The solution of the generalized equations is also given in a form of dispersion features such as phase and group velocity dispersion curves and mode shapes. Each of these features is discussed with emphasis on their usage in wave mode selection issues and importance for application area.

In this chapter, the basic theory of the Semi-Analytical Finite element method for solving guided wave problem in multilayered plate like structure will be introduced. Modeling issues and solution of this method for obtaining dispersion features are also discussed under the “Post-processing” section. The solution of resulting eigen-value problem, consisting of all modes (propagating, evanescent and non-propagating) and their dispersion relation will be given in detail for considering perfectly elastic and damped medium types.

4.1 Definition of SAFE Method for Guided Waves

As mentioned before, (Bartoli et al., 2006) ,(Rose 2014), (Van Velsor 2009), and (M.Mazzotti 2013), this method is based on an analytical solution of the propagating wave direction while the finite element discretization domain is perpendicular to this propagating wave direction. In order to define guided wave propagation on the waveguide, exponential time harmonic wave assumption ($e^{i(kx-\omega t)}$) can be employed with the propagation direction (x), wavenumber (k), angular frequency ($w = 2\pi f$) and time (t).

Considering a multilayered plate model in xy - plane on Cartesian coordinate system, stress, strain and displacement relations with corresponding indices can be given at individual points on a plate by;

$$\begin{aligned}
u &= [u_x \quad u_y \quad u_z]^T \\
\varepsilon &= [\varepsilon_{xx} \quad \varepsilon_{yy} \quad \varepsilon_{zz} \quad \varepsilon_{yz} \quad \varepsilon_{xz} \quad \varepsilon_{xy}]^T \\
\sigma &= [\sigma_{xx} \quad \sigma_{yy} \quad \sigma_{zz} \quad \sigma_{yz} \quad \sigma_{xz} \quad \sigma_{xy}]^T
\end{aligned}
\tag{4.1}$$

where, ‘ T ’ represents transpose of these matrices. For applying finite element procedure on perpendicular domain which lies yz -plane of the waveguide is divided in small finite elements. Each of these elements can be represented with 1-dimensional quadratic shape functions for the thickness direction (z) since we assume multilayered plate model to be infinite in y -direction. The detailed explanation of this type of shape functions and usage in finite element discretization methods can be found in (Cook 2001) book.

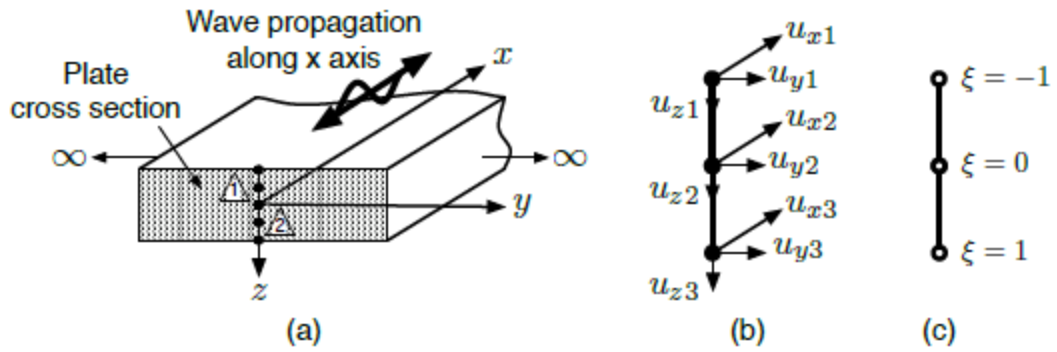


Figure 4.1. Representation of infinitely long plate model in (y) direction with discretization on the plate thickness with 2 quadratic line elements (a), Degrees of freedom for each displacement and direction (b), At each elements individual location of isoparametric element (c).

(Source: ‘ (Ahmad 2011)’)

This multilayered plate model is shown in the Figure (4.1). Each element mapped with isoparametric elements (ξ), whose individual locations are $\xi = (-1, 0, 1)$ used for each line element respectively. The nodes and their corresponding shape functions are also designed with indices 1, 2 and 3.

For a given point, the global coordinate (z) can be found by using shape functions in local coordinates and corresponding global coordinates (z_1, z_2, z_3) of these three nodes. This relation can be shown in matrix form as in equation (4.2)

$$z = [N_1 N_2 N_3] \begin{bmatrix} z_1 \\ z_2 \\ z_3 \end{bmatrix} \quad (4.2)$$

where, shape functions of each node are given in equation (4.3)

$$\begin{aligned} N_1 &= \frac{1}{2}(\xi^2 - \xi) \\ N_2 &= (1 - \xi^2) \\ N_3 &= \frac{1}{2}(\xi^2 + \xi) \end{aligned} \quad (4.3)$$

As can be seen from the figure (4.1) each node has three degrees of freedom which are defined in three principal displacement directions. Using the same procedure in equation (4.2), three particle displacement components of each element considering harmonic wave propagation in x-direction can be shown in terms of each nodal displacements and shape functions as in equation (4.4);

$$u^{(e)} = \begin{bmatrix} u_x^{(e)} \\ u_y^{(e)} \\ u_z^{(e)} \end{bmatrix} = \begin{bmatrix} \sum_{l=1}^3 N_l(\xi) U_{xl} \\ \sum_{l=1}^3 N_l(\xi) U_{yl} \\ \sum_{l=1}^3 N_l(\xi) U_{zl} \end{bmatrix} e^{i(kx - \omega t)} = N(\xi) q^{(e)} e^{i(kx - \omega t)} \quad (4.4)$$

where, shape function matrix is given in equation (4.5) like;

$$N(\xi) = \begin{bmatrix} N_1 & 0 & 0 & N_2 & 0 & 0 & N_3 & 0 & 0 \\ 0 & N_1 & 0 & 0 & N_2 & 0 & 0 & N_3 & 0 \\ 0 & 0 & N_1 & 0 & 0 & N_2 & 0 & 0 & N_3 \end{bmatrix} \quad (4.5)$$

And, nodal displacements matrix is given by;

$$q^{(e)} = [U_{x1} \quad U_{y1} \quad U_{z1} \quad U_{x2} \quad U_{y2} \quad U_{z2} \quad U_{x3} \quad U_{y3} \quad U_{z3}]^T \quad (4.6)$$

In equation (4.6), x, y and z represent direction; and 1, 2 and 3 are the node numbers on each element. After finding the nodal displacements at each directions x, y and z, substituting equations (3.2) and (3.3) from previous chapter, the strain and the stress relations for each elements can be represented in matrix form as;

$$\varepsilon^{(e)} = \begin{bmatrix} \varepsilon_{xx} \\ \varepsilon_{yy} \\ \varepsilon_{zz} \\ \varepsilon_{yz} \\ \varepsilon_{xz} \\ \varepsilon_{xy} \end{bmatrix} = \begin{bmatrix} \frac{\partial}{\partial x} & 0 & 0 \\ 0 & \frac{\partial}{\partial y} & 0 \\ 0 & 0 & \frac{\partial}{\partial z} \\ 0 & \frac{\partial}{\partial z} & \frac{\partial}{\partial y} \\ \frac{\partial}{\partial z} & 0 & \frac{\partial}{\partial x} \\ \frac{\partial}{\partial y} & \frac{\partial}{\partial x} & 0 \end{bmatrix} \times \begin{bmatrix} u_x^{(e)} \\ u_y^{(e)} \\ u_z^{(e)} \end{bmatrix} \quad (4.6)$$

$$\sigma^{(e)} = C^{(e)} \varepsilon^{(e)} \quad (4.7)$$

where, $C^{(e)}$ is the material stiffness matrix which is obtained for isotropic medium by inserting equation (3.2) relations. This matrix then can be reduced to employ only two material constants which are Lamé parameters (λ) and (μ), in a compact matrix form stress-strain relations, which can be written as;

$$\begin{bmatrix} \sigma_{xx} \\ \sigma_{yy} \\ \sigma_{zz} \\ \sigma_{yz} \\ \sigma_{xz} \\ \sigma_{xy} \end{bmatrix} = \begin{bmatrix} \lambda + 2\mu & \lambda & \lambda & & & \\ \lambda & \lambda + 2\mu & \lambda & & & \\ \lambda & \lambda & \lambda + 2\mu & & & \\ & & & 2\mu & & \\ & & & & 2\mu & \\ & & & & & 2\mu \end{bmatrix} \times \begin{bmatrix} \varepsilon_{xx} \\ \varepsilon_{yy} \\ \varepsilon_{zz} \\ \varepsilon_{yz} \\ \varepsilon_{xz} \\ \varepsilon_{xy} \end{bmatrix} \quad (4.8)$$

After, obtaining stress and strain relation for each nodal element by using Hooke's Law, strain-displacement relation for the case of three displacement directions can be written in more simplified form in equation (4.9) by rearranging on differentiation components.

$$\varepsilon^{(e)} = \left[L_x \frac{\partial}{\partial x} + L_y \frac{\partial}{\partial y} + L_z \frac{\partial}{\partial z} \right] u^{(e)} \quad (4.9)$$

where L_x , L_y and L_z given in matrix form;

$$L_x = \begin{bmatrix} 1 & 0 & 0 \\ 0 & 0 & 0 \\ 0 & 0 & 0 \\ 0 & 0 & 0 \\ 0 & 0 & 1 \\ 0 & 1 & 0 \end{bmatrix} \quad L_y = \begin{bmatrix} 0 & 0 & 0 \\ 0 & 1 & 0 \\ 0 & 0 & 0 \\ 0 & 0 & 1 \\ 0 & 0 & 0 \\ 1 & 0 & 0 \end{bmatrix} \quad L_z = \begin{bmatrix} 0 & 0 & 0 \\ 0 & 0 & 0 \\ 0 & 0 & 1 \\ 0 & 1 & 0 \\ 1 & 0 & 0 \\ 0 & 0 & 0 \end{bmatrix} \quad (4.10)$$

Using nodal displacement and harmonic wave assumption in equation (4.4) and substituting this equation into the generalized strain vector $\varepsilon^{(e)}$ in equation (4.8), it can be shown that;

$$\varepsilon^{(e)} = (B_1 + ikB_2)q^{(e)}e^{i(kx-\omega t)} \quad (4.11)$$

where, Strain-Displacement matrices B_1 and B_2 obtained from equation (4.9) are given as follows;

$$\begin{aligned} B_1 &= L_y N_{,y} + L_z N_{,z} \\ B_2 &= L_x N \end{aligned} \quad (4.12)$$

In these expressions, L is given in matrix form in equation (4.10) and $N_{,z}$ and $N_{,y}$ are the derivatives of the shape function matrix $N(\xi)$ given in equation (4.5) with respect to z and y directions respectively. It is also worth noting that since we assumed multilayered plate model to be infinite in (y) direction under this assumption, our problem turns as y invariant and it can be eliminated from the derivation. After making this simplification, B_1 matrix can be calculated from only using L_z and $N_{,z}$ matrices. The derivatives of the shape function $N(\xi)$ with respect to z direction cannot be calculated directly since these shape functions are function of isoparametric elements (ξ). In order to do that, Jacobian matrix should be introduced with respect to z direction. These expressions can be written by applying chain rule as follows;

$$\frac{dN(\xi)}{dz} = \frac{dN(\xi)}{d\xi} \frac{d\xi}{dz} = \frac{1}{J} \frac{dN(\xi)}{d\xi} \quad (4.13)$$

Where Jacobian matrix is given as;

$$J = \frac{dz}{d\xi} = \begin{bmatrix} \xi - \frac{1}{2} & -2\xi & \xi + \frac{1}{2} \end{bmatrix} \begin{bmatrix} z_1 \\ z_2 \\ z_3 \end{bmatrix} \quad (4.14)$$

4.2 Hamilton's Principle

In order to derive the equation of motion for discretization domain in SAFE method, these generalized strain and displacement fields from the previous section are implemented in Hamilton's principle with using kinetic and potential energy equilibrium relations, since our system is dynamic and there is no external body force. This assumption is made for conservative systems in here, where there is no energy dissipation out of the system. With considering all these aspects, variation form of Hamiltonian is given as;

$$\delta H = \int_{t_1}^{t_2} \delta(W - K_e) dt = 0 \quad (4.15)$$

This expression is stated that in a time interval between t_1 and t_2 total change of potential or strain energy and kinetic energy variations remains constant. By using this, kinetic energy term can be given as;

$$K_e = 1/2 \int_V \dot{u}^T \rho \dot{u} dV \quad (4.16)$$

In eqn (4.16) ρ is density, u is the displacements, dot “.” representing the time derivative and V is volume. Potential energy or strain energy term W , can also be given as;

$$W = 1/2 \int_V \varepsilon^T C \varepsilon dV \quad (4.17)$$

where T denotes as transpose of strain matrix ε and C is representing material stiffness matrix. In true sense, using conservative form of Hamilton’s principle is extended by (Bartoli, *et al.* 2006) with introducing the complex number in material stiffness matrix C in order to investigate the mediums with loss. As a result, the solution of this equation gives complex values, which consists of both real and imaginary parts. The real parts represent the conserved elastic energy, and the imaginary part of the results stands for the dissipated energy in the system.

Substitution of Eqn (4.16) and Eqn (4.17) into the conservative form of the Hamilton’s principle in Eqn (4.15) and making integration by parts in kinetic energy term results in;

$$\delta H = \int_{t_1}^{t_2} \left[\int_V \delta(u^T) \rho \dot{u} dV + \int_V \delta(\varepsilon^T) C \varepsilon dV \right] dt = 0 \quad (4.18)$$

Recall from the previous section that, strain and displacement relations are obtained for each element along the thickness direction. As a result, the generalized

Hamilton's equation in (4.18) can be rewritten with considering each element in order to define whole system. The discrete form can be written as;

$$\int_{t_1}^{t_2} \left(\bigcup_{e=1}^{n_{el}} \left[\int_V \delta(u^{(e)T}) \rho_{(e)} \ddot{u}^{(e)} dV + \int_V \delta(\varepsilon^{(e)T}) C_{(e)} \varepsilon^{(e)} dV \right] \right) dt = 0 \quad (4.19)$$

Where, n_{el} is representing total number of cross-sectional elements, symbol \bigcup represents the assembly of the all elements in discretization direction, $C_{(e)}$ is the material stiffness matrix of corresponding medium and $\rho_{(e)}$ is density of each elements.

The substitution of strain-displacement expression for each element in Eqn (4.11) into the strain energy part of the conservative form of the Hamiltonian equation and making some simplifications yields;

$$\begin{aligned} \int_V \delta(\varepsilon^{(e)T}) C_{(e)} \varepsilon^{(e)} dV_e = \\ \int_{\Omega_e} \int_x \delta \left((B_1^T - ikB_2^T) q^{(e)T} (e^{i(kx-\omega t)})^T \right) C_{(e)} (B_1 \\ + ikB_2) q^{(e)} e^{i(kx-\omega t)} dx d\Omega_e \end{aligned} \quad (4.20)$$

where the transpose of the imaginary unit in exponential term $i^T = -i$, and with using this equality material stiffness matrix $C_{(e)}$ can be found by integrating over the cross-sectional domain and then, taking the integration with respect to x and taking the all terms in the equation in virtual displacement $\delta q^{(e)T}$ parenthesis yields;

$$\begin{aligned} \int_{\Omega_e} \delta \left((B_1^T - ikB_2^T) q^{(e)T} \right) C_{(e)} (B_1 + ikB_2) q^{(e)} e^{i(kx-\omega t)} dx d\Omega_e \\ = \delta q^{(e)T} \int_{\Omega_e} \left[B_1^T C_{(e)} B_2 - ikB_2^T C_{(e)} B_1 + ikB_1^T C_{(e)} B_2 \right. \\ \left. + k^2 B_2^T C_{(e)} B_1 \right] d\Omega_e \end{aligned} \quad (4.21)$$

This generalized equation satisfies any virtual displacements so this part can be omitted from the equations. The second part of the conservation form of the Hamilton principle is the kinetic energy term. Using the displacement equation (4.4), which is obtained in previous section and substituting this displacement expressions in kinetic

energy terms in equation (4.19) by omitting the exponential terms $e^{i(kx-\omega t)}$ from the both sides of the equation yields;

$$\begin{aligned} \int_V \delta(u^{(e)T}) \rho_{(e)} \ddot{u}^{(e)} dV &= \int_{\Omega_e} \int_x \delta(u^{(e)T}) \rho_{(e)} \ddot{u}^{(e)} dx d\Omega_e \\ &= -w^2 \delta q^{(e)T} \int_{\Omega_e} N^T \rho_{(e)} N d\Omega_e q^{(e)} \end{aligned} \quad (4.22)$$

After that, substituting Eqn (4.21) and (4.22) into the Hamilton's equation for each element can be given as;

$$\int_{t_1}^{t_2} \left(\bigcup_{e=1}^{n_{el}} \delta q^{(e)T} [k_1^{(e)} + i k k_2^{(e)} + k^2 k_3^{(e)} - w^2 m^{(e)}] q^{(e)} \right) dt = 0 \quad (4.23)$$

It is also worth to noting that, at the beginning of the chapter while modelling multilayered structure 1 dimensional shape function with 3 nodes is used for each element. Discretization of the thickness direction is made by using these line elements, which are functions of isoparametric elements (ξ) only. As a result, instead of taking the integration over cross-sectional domain (Ω_e), we can take integration with respect to these isoparametric elements in a similar manner. With considering these aspects in Eqn (4.23) all terms can be simplified as;

$$\begin{aligned} k_1^{(e)} &= \int_{-1}^1 B_1^T C_{(e)} B_2 d\xi \\ k_2^{(e)} &= \int_{-1}^1 (B_1^T C_{(e)} B_2 - B_2^T C_{(e)} B_1) d\xi \\ k_3^{(e)} &= \int_{-1}^1 B_2^T C_{(e)} B_1 d\xi \\ m^{(e)} &= \int_{-1}^1 N^T \rho_{(e)} N d\xi \end{aligned} \quad (4.24)$$

After that, applying standard finite element assembling procedure for all elements with considering traction free boundaries at bottom and top surface of the plate structure. Wave equation for the total system can be obtained as follow;

$$T^T K_1 T = K_1, \quad T^T K_3 T = K_3, \quad T^T K_2 T = -i K_2, \quad T^T M T = M \quad (4.29)$$

Substituting all these matrices into the generalized wave equation in equation (4.27) gives the final form of the quadratic eigen value problem;

$$[K_1 + kK_2 + k^2K_3 - w^2M]_{3N \times 3N} \hat{Q} = 0 \quad (4.30)$$

where, the nodal displacement vector is $\hat{Q} = TQ$. This generalized equation can be reduced in first order Eigen-value system.

$$[A - kB] \begin{bmatrix} \hat{Q} \\ k\hat{Q} \end{bmatrix} = 0 \quad (4.31)$$

where, A and B matrices are;

$$A = \begin{bmatrix} 0 & K_1 - w^2M \\ K_1 - w^2M & K_2 \end{bmatrix} \\ B = \begin{bmatrix} K_1 - w^2M & 0 \\ 0 & -K_3 \end{bmatrix} \quad (4.32)$$

In general case, the numerical solution of this linearized eigenvalue problem gives $6N \times 6N$ size diagonal matrix for eigenvalues and corresponding same size full eigenvector matrix since the reduction in first order system yields doubling the size of matrices. The resulting of eigenvalues gives relations about angular frequency w and wavenumber k pairs, which are the only unknown variables and corresponding eigenvectors \hat{Q} gives the knowledges about the mode shapes or other terms wave structures of propagating waves.

4.3 Post Processing of Eigenvalue Problem

In order to solve this problem, there are two different ways: frequency (w) domain solution and wavenumber (k) domain solution. As mentioned below, post

processing of the eigen value problem is performed by using Eqn (4.32) with giving the frequency as an input.

Considering an isotropic elastic plate model, which is defined by real-valued Lamé parameters λ and μ as material properties in stiffness matrix C and 1-D line elements for discretization on thickness direction consists of N nodes. Eigen solution of each real frequency (w) gives $6N$ real eigenvalues for wavenumber (k) which are included both forward ($+x$) and backward ($-x$) wave motion. Positive wavenumber solution “ $+k$ ” represents the forward wave motion and negative wavenumber “ $-k$ ” is representing backward wave motion. These resulting wavenumber solutions are used describing calculate the velocity of the propagating waves in a form of phase velocity dispersion curve as done in previous chapter. On the other hand, when dealing with attenuative media (damped medium), complex values solution should be considered. As a result, eigen solution of the system results in complex eigenvalues and corresponding complex eigenvectors. These resulting wavenumber and their conjugate complex pairs can be given in the form of $k = \pm k_{real} \pm ik_{im}$, which includes all possible wave modes in both forward and backward directions. The wavenumber solution should be processed to make a distinction on propagating, non-propagating and evanescent wave modes. A good review of distinction on wave modes can be found in (Mazzotti 2013) section 2.6. In these general forms of the solutions, real part of the wavenumber solution $\pm k_{real}$ represents propagating waves in both directions ($\pm x$). The complex wavenumber solution represents the evanescent wave modes. Separation of wave modes from each other can be made by following considerations. When, both real and imaginary parts of the complex wavenumber k_{real} and k_{im} are greater than zero, the wave mode can be said to propagate in ($+x$) direction with attenuation. In contrast, if the imaginary part of the wavenumber is smaller than zero this corresponds to a wave mode propagating in ($-x$) direction with attenuation. In addition to that, if obtained wavenumber solutions consist of only imaginary $\pm ik_{im}$ values, these wave modes can be said to be non-propagating waves.

After distinction of all this modes, with selecting wave propagation direction, the total system of wave motion solution can be yield. These obtained and selected propagating wave modes and their solution as the wavenumber (k) at each frequency are used to generate the phase velocity dispersion curves.

4.3.1 Group Velocity Concept

As stated previously, the group velocity can be derived after obtaining phase velocity of each wave modes, and by taking the differentiation. This numerical differentiation can cause some large errors if the frequency step is selected large. However, in SAFE method the group velocity of the propagating waves can be derived directly from the eigen solution results as proposed by (Finnveden 2004) and following with the (Bartoli, 2006). This method is started with taking the derivative of Eqn (4.30) with respect to wavenumber (k) as follows;

$$\frac{\partial}{\partial k} [K(k) - w^2 M] \hat{Q}_R = 0 \quad (4.33)$$

Here, $K(k) = K_1 + kK_2 + k^2K_3$ and \hat{Q}_R is representing the right eigen vector which can be solved from the Eqn (4.31) directly. Then, pre-multiplying the obtained equation (4.33) with the transpose of the left eigen vector \hat{Q}_L^T , which can be found from solving the generated wave equations with introducing transpose of the matrix A and B in Eqn(4.32) as follows.

$$[A^T - kB^T] \hat{Q}_L = 0 \quad (4.34)$$

After substituting Eigen vector solutions, derived equation in can be rewritten as;

$$\hat{Q}_L^T \left[\frac{\partial}{\partial k} (K_1 + kK_2 + k^2K_3) - 2w \frac{\partial w}{\partial k} M \right] \hat{Q}_R = 0 \quad (4.35)$$

Then, taking the derivatives of stiffness matrices with respect to k and keeping in mind that differentiation of the frequency (w) with respect to wavenumber (k) results in scalar quantities, the group velocity dispersion relation yields;

$$C_g = \frac{\partial w}{\partial k} = \frac{\hat{Q}_L^T (K_2 + 2kK_3) \hat{Q}_R}{2w \hat{Q}_L^T M \hat{Q}_R} \quad (4.36)$$

This derived equation shows that group velocity of propagating wave mode can be calculated by using each wavenumber k and frequency $\omega = 2\pi f$ solutions since it is only a function of (k, ω) pairs. There is no need to take derivative by using the phase velocity computation for each frequency. As a result, this method provides more robust and reliable way of the illustrating the group velocity dispersion relations.

Another dispersion feature is mode shapes of propagating waves along the thickness directions as stated before. In analytical solution which is summarized in previous chapter, computation of mode shapes of the propagating waves requires the more computations. However, in SAFE method, the mode shape information can also directly be obtained from eigen vector results.

Recall from the formulation in equation (4.31), numerically calculation of these wave equations at each frequency in the range of interest gives the all propagating wave modes solution as wavenumber (k). This solution can be used for illustrating the mode shapes of desired wave modes at specified frequency points as well. The corresponding eigen-vector results consist of the mode shapes information of the desired wave after selecting the wave mode solution. Based on this mode shape solution, stress and strain distribution can be calculated using equation (4.6) and (4.7), since the resulting eigen-vectors are formulated as nodal displacement vectors.

CHAPTER 5

SAFE METHOD NUMERICAL EXAMPLES

In this section, the SAFE method described in the previous section will be solved numerically for considering single layer plate and multilayered structures. The resulting dispersion relations in terms of phase velocity, group velocity dispersion curves of propagating waves will be present. Parameters for modelling the selected examples will also be covered. The validity of the results will be evaluated taking into account the results of previous studies and analytical matrix-based solution methods. To do this, the results of the DISPERSE software program will be used first. In order to perform the numerical solution, all SAFE formulation is implemented in MATLAB 2014b program and generalized eigen value problem in equation (4.31) are solved with using ‘*eig*’ function, which is capable of calculating eigen solutions in both real and complex number domains. It is also worth to noting that while using the FEM approach, the convergence of the solution is crucial situation in order to get more accurate results. This issue arises from the numerical approximation on interpolation (shape) functions used in discretization. As in SAFE solution this convergence situation will be handled with increasing the number of elements. In order to do that smallest wave length assumption was considered for whole medium as first. The total number of nodes which is getting the more accurate results can be calculated (Van Velsor 2009) as follows;

$$NoN = \frac{NoExf_{max}xTh}{c_{sl}} \quad (5.1)$$

In this equation, *NoN* is representing the number of total nodes, *NoE* is representing the number of nodes in each element while using the discretization of domain, *Th* is representing the total thickness of the multi layered configuration. *c_{sl}* is representing the lowest shear bulk wave velocities among all different medium, since the propagating lowest phase velocity of whole system can be estimated from that medium which has lower shear bulk wave velocity. In addition to that, all the analyses are performed by giving the desired frequency range with small frequency increments

about 0.05. All the studies which are presented in here are applied to SAFE formulations with considering those relations.

5.1 Case Study-1

In this case studies, SAFE method solutions are compared with the Disperse program results. A single layer isotropic structure configuration is used for generate the dispersion features first. The material properties are also taken from Disperse program for comparison. In the first example, isotropic single layer system was considered and analysis was made on a 2 mm thickness titanium plate model whose material properties and acoustic properties were given in Table (5.1). While making the discretization along the thickness direction of the model, 1-Dimensional 3 nodes line elements was used. The resulting dispersion features were presented only considering Lamb wave modes where the total solution of system are decoupled from the u_y direction as mentioned previous section. This means that, only u_x and u_z displacements should be used in that solution. In analysis, 62 elements which is consist of 186 nodes were used with taking into account of smallest wave assumption in equation (5.1), only 124 of them was considered which are corresponding to desired Lamb wave modes in this solution.

5.1.1 Results

The resulting Lamb wave modes up to 5-Mhz for both methods in a form of phase velocity dispersion curve and group velocity dispersion curves results are also given in Figure (5.1) and Figure (5.2) respectively.

Table 5.1. Material and acoustic properties of Titanium plate

Material	C_l (m/s)	C_s (m/s)	ρ kg/m^3	h mm
Titanium	6060	3230	4460	2

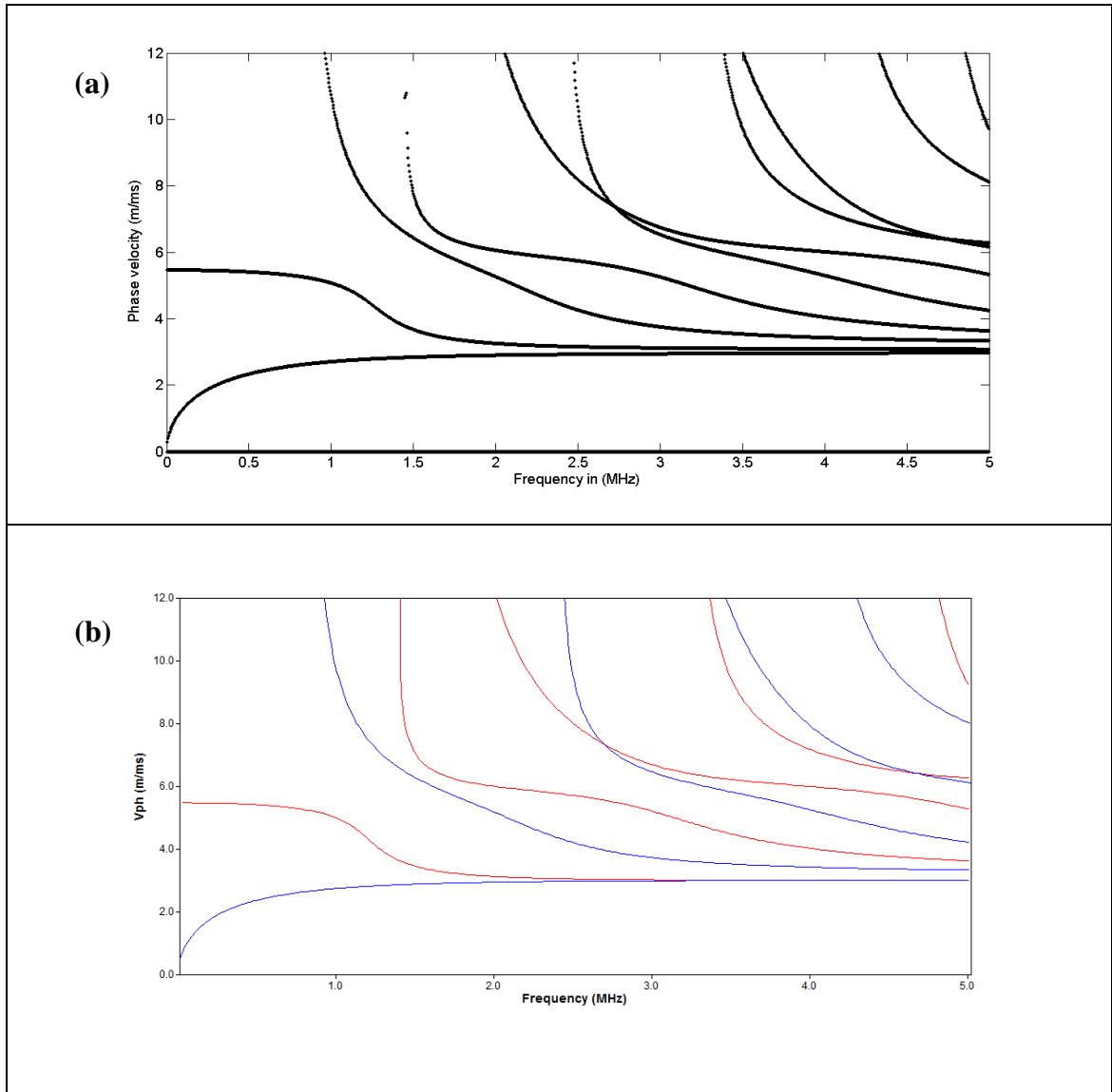


Figure 5.1. Phase velocity Dispersion curve of 2-mm thickness titanium plate structure results for SAFE (a) and for GMM (b). Red line for symmetric modes, blue line for asymmetric wave modes.

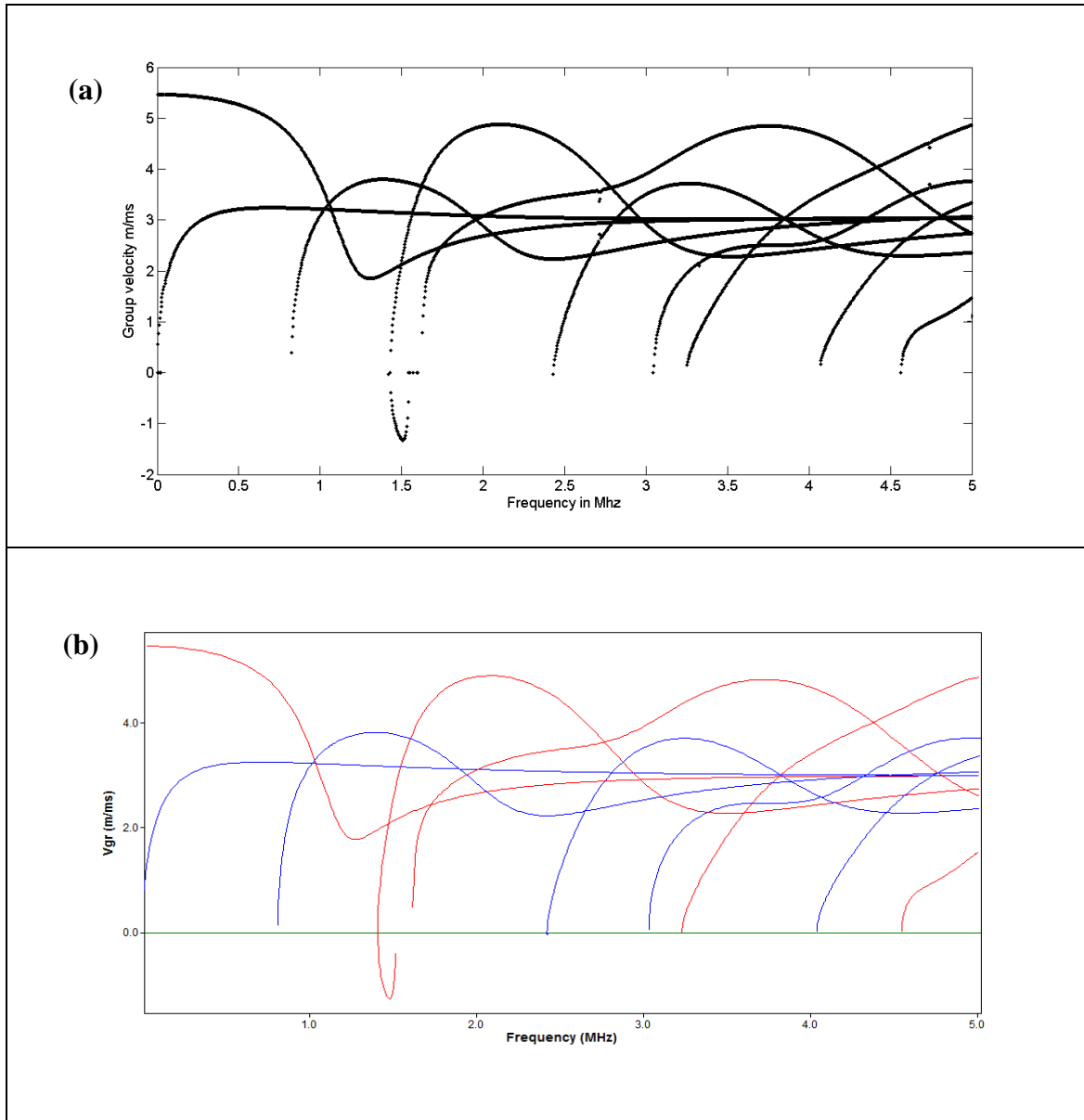


Figure 5.2. Group velocity Dispersion curve of 2-mm thickness Titanium plate structure results for SAFE (a) and for GMM (b). Red line for symmetric wave modes, blue line for asymmetric wave modes.

The comparison of these two methods on isotropic model was made by selecting 4 sample points on obtained phase velocity dispersion curves. In order to do that, instead of investigate whole obtained frequency spectrum only up to 1.4 MHz were analyzed which are consisted of only zero order symmetric (S_0) and asymmetric (A_0) Lamb wave modes. These selected points were illustrated on Figure (5.3) which was obtained phase velocity dispersion curve from SAFE approach.

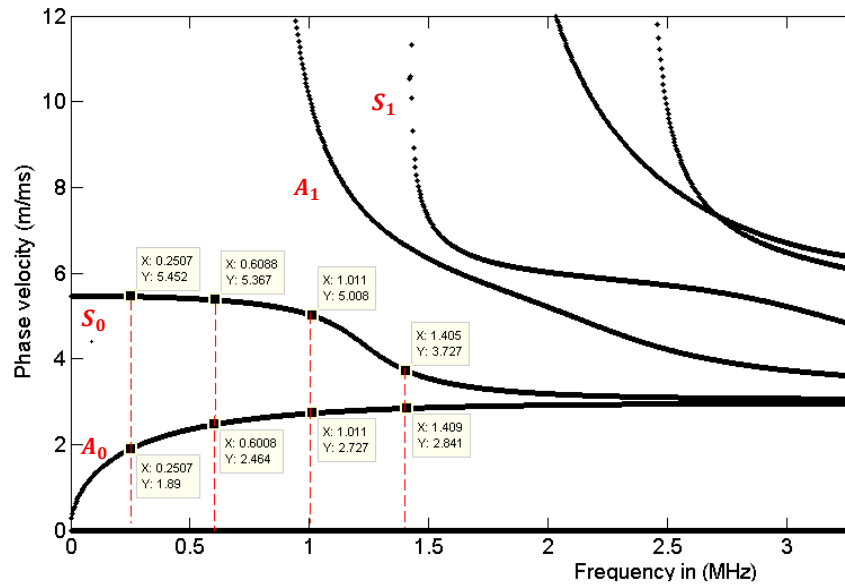


Figure 5.3. Schematic representation of the phase velocity values corresponding to the four selected frequency values on symmetric and antisymmetric wave modes obtained using the SAFE method

The results obtained from both methods at selected frequency points are listed in Table (5.2), for zero order Symmetric and Asymmetric wave modes in Table (5.3), GMM results are obtained from using the Disperse software directly. The reason of selecting these lower order wave modes comes from the fact that, in lower frequency spectrum and corresponding lower order wave modes carry more energy compared with other modes and of most importance. In a practical application, to inspected the desired structure for long range those wave modes are widely used (Juluri 2008), (Fan 2010) and etc. Another reason of using lower order wave modes in real application is that, studying on the low frequency range leads to include only a few wave modes to propagate in the inspected structure. As a result, the separation of reflected wave modes from discontinuities and cracks in the inspected medium can be done easily during measurements.

Table 5.2. Comparison of the phase velocities of GMM and SAFE methods at four different frequency values for symmetrical zero order (S_0) wave mode on a 2 mm thickness Titanium Plate

Phase Velocity for S_0 modes	0.25 MHz	0.60 MHz	1.0MHz	1.4MHz
SAFE (m/ms)	5.451	5.401	5.000	3.727
Disperse GMM (m/ms)	5.450	5.402	4.988	3.704
Error	0.018 %	0.018 %	0.24 %	0.62 %

Table5.3. Comparison of the phase velocities of GMM and SAFE methods at four different frequency values for symmetrical zero order (A_0) wave mode on a 2 mm thickness Titanium Plate

Phase Velocity for A_0 modes	0.25 MHz	0.60 MHz	1.0MHz	1.4MHz
SAFE (m/ms)	1.897	2.464	2.727	2.841
Disperse GMM (m/ms)	1.902	2.473	2.734	2.857
Error	0.262 %	0.363 %	0.256 %	0.56 %

5.2 Case Study-2

As second example, the analysis is performed for three layered system, which consists of an epoxy layer embedded in-between aluminum plates. These types of structure are highly encountered in aerospace industry in order to reduce the vibrational effects as they have good damping characteristics and also light weights. Geometric modelling and material properties of the structure are listed in Table (5.4) and taken from the (Birgani *et al.* 2015). In this paper this configuration is studied based on the GMM and effects of the viscoelastic medium is adopted for the solution with using Kelvin-Voigt model. This multilayered configuration consists of two elastic layers and one viscoelastic layer. In order to investigate wave propagation in losses media with SAFE, it is necessary to first determine the complex material stiffness matrix for the

solution. This model is referred as a hysteretic model where the complex Lamé parameters are consisted of both storage and loss modulus of related material in order to defining the damped. This model is proposed by (Bartoli *et al.* 2006). Following this reference, the complex elastic parameters of the material can be found as follows to introduce damping to the system;

$$c_{l,s} = c_{l,s} \left(1 + i \frac{k_{l,s}}{2\pi} \right)^{-1} \quad (5.2)$$

where, $c_{l,s}$ are representing the complex longitudinal and shear bulk wave velocities and $k_{l,s}$ are the corresponding wavenumbers. Then, using these velocities the complex Young's modulus (E) and Poisson's ratio (ν) are obtained as follows;

$$E = \rho C_s^2 \left(\frac{3c_l^2 - 4c_s^2}{c_l^2 - c_s^2} \right) \text{ and } \nu = 1/2 \left(\frac{c_l^2 - 2c_s^2}{c_l^2 - c_s^2} \right) \quad (5.3)$$

These expressions, in the form of complex Young's modulus and Poisson's ratio, are used to obtain complex Lamé parameters for viscoelastic medium from using Equation (3.18) and then the complex stiffness matrix C is formed by using these parameters. By using this model, the complex stiffness matrix is formed for desired attenuative medium only once for analysis of the multilayered structures. The difference between Kelvin-Voigt model and hysteretic model is that, Kelvin-Voigt model has a frequency dependent loss modulus and it should be updated for each frequency during the analysis. This makes the analysis more complicated. For that reason, in the case studies, presented damping model is adopted for the SAFE solution.

Table 5.4. Geometric and Acoustic properties of Elastic–Viscoelastic-Elastic Multilayered structure

Layer	Material	C_l (km/s)	α_l (s/km)	C_s (km/s)	α_s (s/km)	ρ g/cm ³	h mm
1	Aluminum	6.35	-	3.13	-	2.7	1.6
2	Epoxy 303	2.39	0.0070	0.99	0.0201	1.08	0.66
3	Aluminum	6.35	-	3.13	-	2.7	3.175

As mentioned earlier, attenuation magnitude on wave propagation is a crucial issue for inspecting the structure through long distances. Selection of the less attenuated wave modes leads to more inspecting distance. This quantity can be explained by decreasing the wave amplitude with distance for both bulk wave velocities, α_l is the longitudinal wave attenuation and α_s is the shear wave attenuation. With taking into account of this relation, the desired wave mode attenuation magnitude was calculated by obtaining the imaginary part of the eigen solutions. In order to do that, the resulting imaginary part of the wavenumber solution (k_{im}) was converted to decibel unit using the equation as follows.

$$\alpha_{att} = 20 \log_{10} e^{(-1000 * k_{im})} \quad (5.4)$$

By using this equation (5.4) attenuation level (α_{att}) was considered as decibel per unit length ($dB \text{ meter}^{-1}$) for propagating wave in the medium. With considering all these aspects, the dispersion results obtained from the SAFE method of desired multilayered model are shown in Figure (5.4)

5.2.1 Results

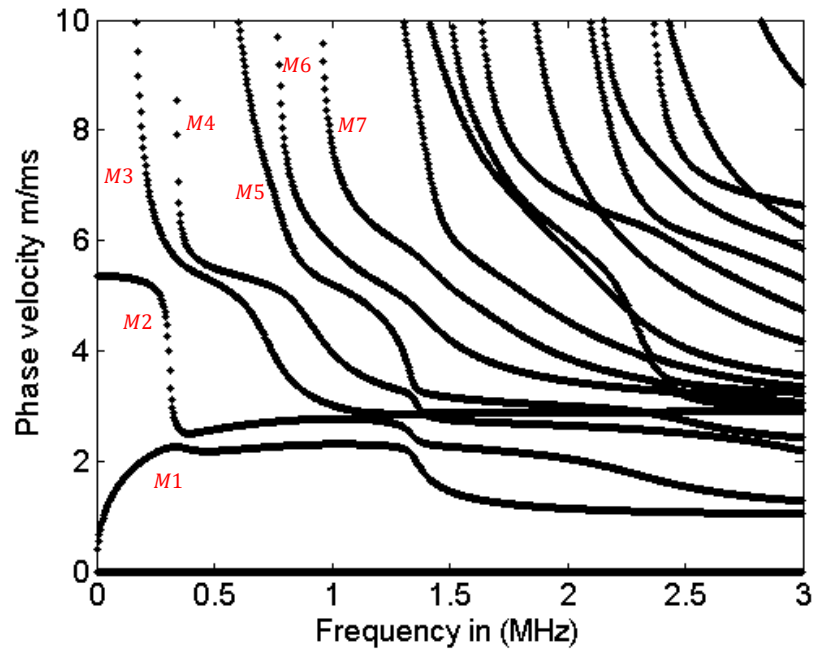


Figure 5.4. Phase velocity dispersion curve of 3-layered elastic-viscoelastic-elastic obtained from SAFE

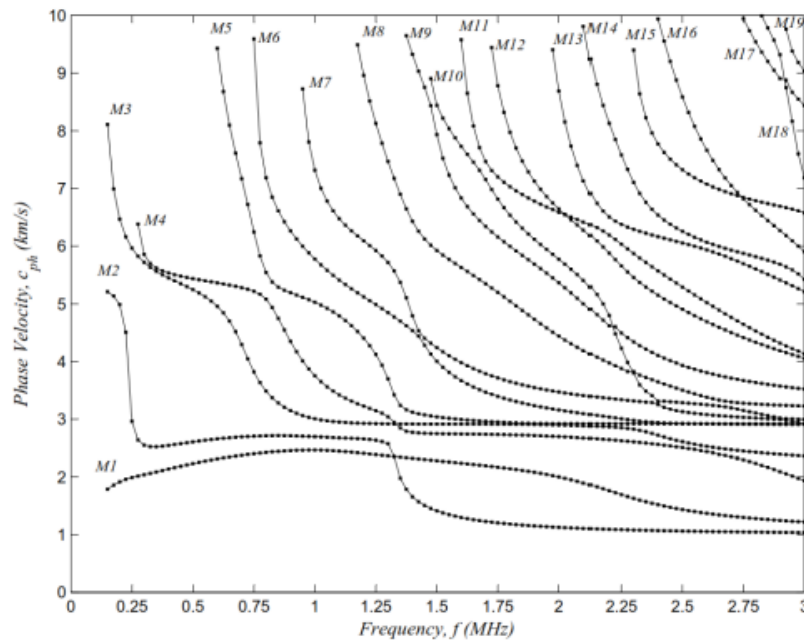


Figure 5.5. Phase velocity dispersion curve results of 3-layered system from GMM
(Source: Birgani *et al.*, 2015)

Figure (5.4) and Figure (5.5) shows the phase velocity dispersion curve of multilayered elastic-viscoelastic model at desired range of frequency. These dispersion results are made based on SAFE and GMM, respectively. The resulting dispersion curves are illustrated the Lamb wave modes similar to the previous example. As can be seen from the Figure (5.4) and (5.5), the phase velocity dispersion curves obtained from the multilayer modeling with SAFE are match well with the GMM results which is taken from the reference paper. When these curves were examined, it appears that only 3 wave modes with a frequency range below 340 kHz propagate through multilayered system. This frequency is cut off frequency of M4 wave mode. Likewise, if the frequency range is below 630 kHz, 4 different wave modes can propagate. This frequency is the value of cut-off frequency for mode 5. For the case of the attenuation level, investigation was made only below the -30 dB/m range with using the expression in equation (5.4) and up to 1-MHz frequency range which is the cut-off frequency of M7 mode are illustrated in Figure (5.6), since that attenuation level is acceptable to present the less attenuated wave mode selections. As can be seen from the Figure (5.4) up to 340 kHz only 3 wave modes can propagate in that medium. These are M1, M2 and M3 wave modes as shown in Figure (5.4).

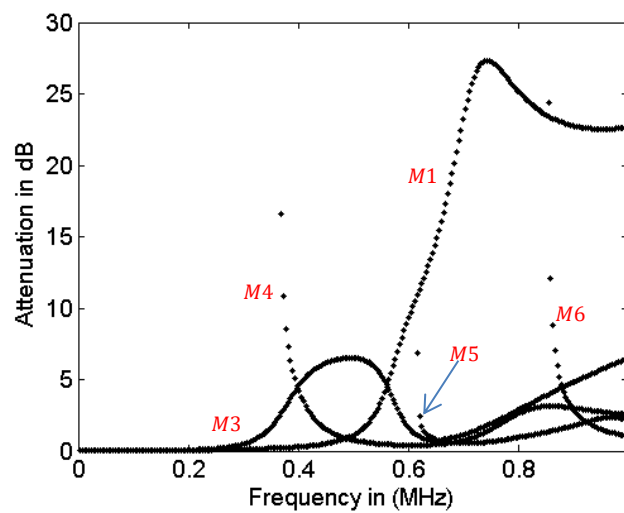


Figure 5.6. Attenuation dispersion curve obtained from SAFE method

The M1 wave mode in the frequency range up to 0.5 kHz has a suitable attenuation level for inspection, as can be seen from the Figure (5.6). For frequencies higher than 0.5 MHz, a sudden increase in the attenuation level is observed. As a result, this wave mode at the higher frequencies above 0.5 MHz is not a suitable choice for

inspection. Another wave mode that propagate through the multilayered medium up to 0.5 MHz is M2 mode. This wave mode can be seen in the phase velocity dispersion curve in Figure (5.4) clearly. At 0.340 MHz, this attenuated wave mode in the viscoelastic structure appears to have a sharp decrease in phase velocity. The sharp decrease in the wave mode shows that very high attenuation occurs on that mode. Since the obtained attenuation curve is shown up to -30 dB/m. These wave modes can not be shown on attenuation curve in Figure (5.6). The measured attenuation at 0.275 MHz for this wave mode is approximately -225 dB/m. For this reason, M2 wave mode is not a suitable mode for inspection. In M3 mode, the frequency range in between 0.280 MHz to 0.660 MHz has an acceptable attenuation level; maximum obtained attenuation is about -5.16 dB per meter in that range. As a result, M3 mode is suitable wave modes for making inspection.

5.3 Case Studies-3

In the previous case studies, SAFE method results are compared with the analytical matrix based solution method. In the first study, single layer isotropic elastic structure is used and obtained results are compared with Disperse program as mentioned before. The modelling issues on the Lamb wave propagation with SAFE method are discussed and analysis results are shown with considering number of usage elements in model. In this study, the analysis is performed on multilayered system in order to investigate the effect of the viscoelastic layer on phase velocity dispersion curve. This conceptual study is designed on three layered symmetric system where viscoelastic layer is embedded in between two aluminum plates which are having the same thicknesses. The material and acoustic properties of the designed system are taken from previous case study and given in below Table (5.5).

Table 5.5. Acoustic and material properties of multilayered system

Layer	Material	C_l (km/s)	α_l (s/km)	C_s (km/s)	α_s (s/km)	ρ g/cm ³
1	Aluminum	6.35	-	3.13	-	2.7
2	Epoxy 303	2.39	0.0070	0.99	0.0201	1.08
3	Aluminum	6.35	-	3.13	-	2.7

In order to perform this analysis and investigated the effects of this loss medium on propagating guided wave modes, the thickness of the viscoelastic layer are increased and given as a thickness ratio (T_{ratio}) which is calculated by dividing the viscoelastic layer thickness (T_{vl}) to the total thickness of the system which is selected as 3-mm. All the analyses are performed up to 5-MHz. Besides this, the number of elements used in each case is kept same for making more reasonable comparison after desired convergence reached. At each case obtained phase velocity results from the SAFE method are also shown below in Figure (5.7)

Table 5.6. Thickness ratios for viscoelastic layer embeded with two elastic plates

$(T_{ratio}) = (T_{vl}) / (T_{total})$	(a)	(b)	(c)	(d)
	0.66	0.53	0.4	0.25

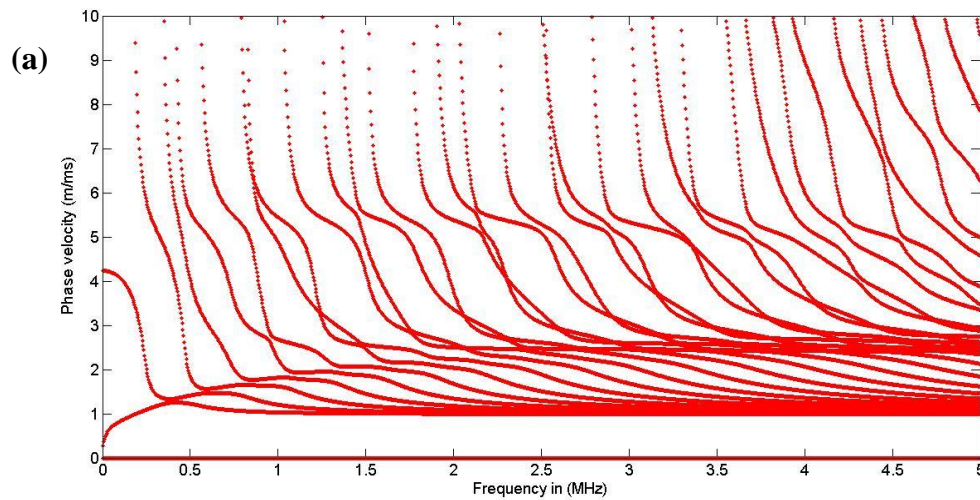
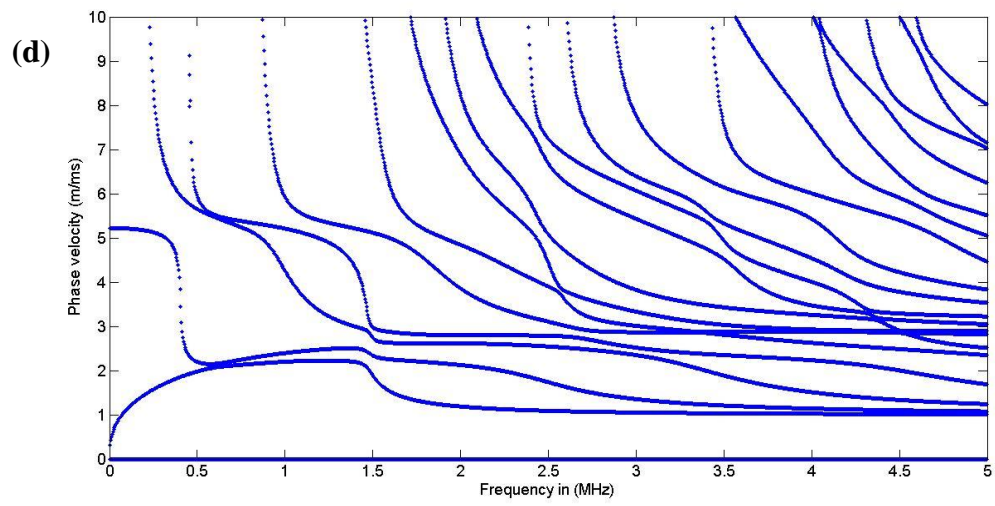
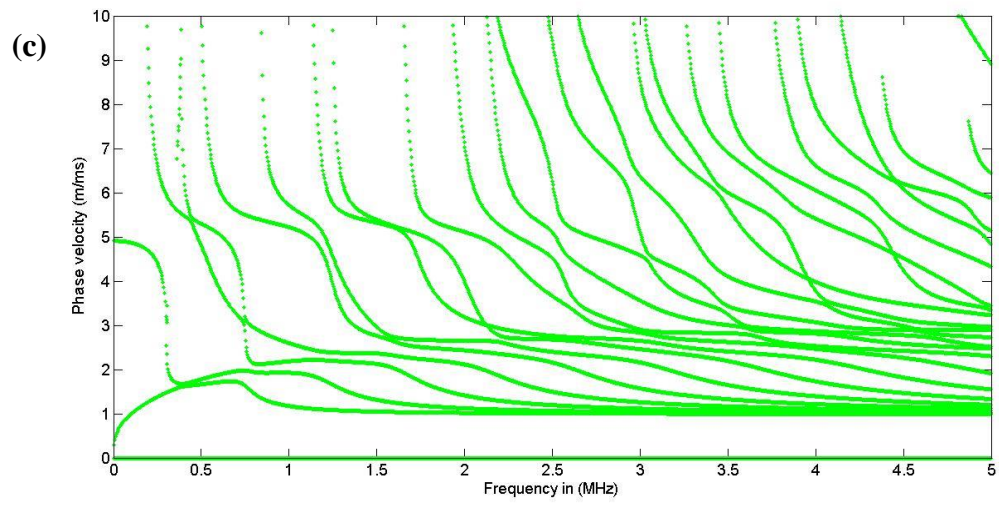
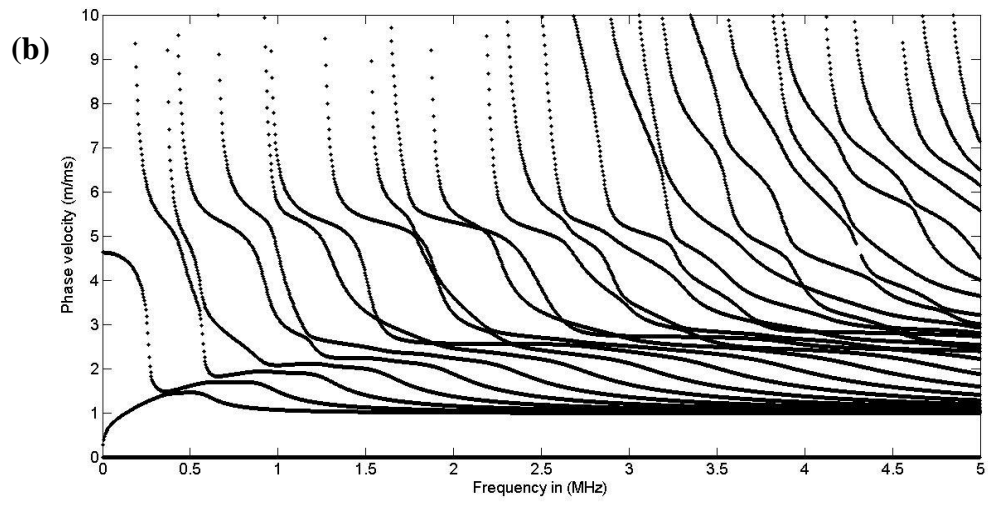


Figure 5.7. Phase velocity dispersion curve of the 3-layered symmetric system with vary thickness ratio of viscoelastic layer embeded between two aluminum plates. Thickness ratio for (a)=0.66 ,(b)=0.53 , (c)=0.4 ,(d)=0.25 (**cont. on next page**)



As can be seen from the Figure (5.7) the effects of the viscoelastic layer thickness on phase velocity dispersion curve are shown in four different thicknesses ratio. It was clearly seen that, although the total thickness of the system remains constant, the number of propagating wave modes are increased in the same frequency range. On the other hand, the number of propagating modes is an only function of frequency on the same thickness plates. The differences between these two situations comes from the dissipation of the wave energy in viscoelastic medium. This energy dissipation is caused more wave modes to propagate in the system. In practical application, determining of the reflected wave modes from the cracks or discontinuities is getting complex issue due to the increasing number of the propagating wave modes.

Other effects of the viscoelastic layer thickness increases can be estimated by examining the phase velocity values of the same frequency points. In order to have a better explanation of this, obtaining phase velocity dispersion curves for the each case are imposed on the same Figure (5.8), and shown up to 0.75-MHz frequency.

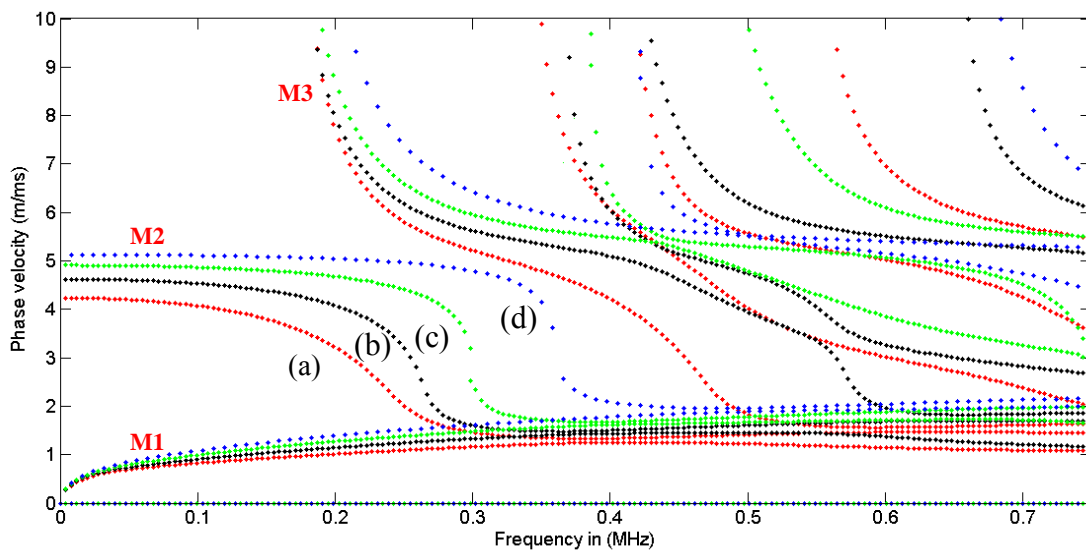


Figure 5.8. Different viscoelastic layer thickness results on same Phase velocity dispersion curve of three layered system

As can be seen from the Figure (5.8), the viscoelastic layer thickness increases are more influential on M2 and other wave modes compared to M1. This influence is clearly seen between the frequencies 0.220 to 0.375 MHz. For the thickness ratio 0.25 which is represented in curve (d), due to lower viscoelastic medium thickness, phase velocity of the M2 wave modes almost remains constant up to 0.375 MHz, and then sharp decrease is observed due to wave propagation with attenuation. When the

thickness ratio is 0.66, it was clearly seen from the curve (a) phase velocity of M2 mode was starts to decrease in smaller frequency values. As a result, the instability behaviour of the propagating M2 modes in terms of phase velocities showed that, in the practical applications, large error could be induced on that frequency bandwindth, where the phase velocity values changes sharply. For this reason, more stable frequency regions in terms of the phase velocity changes could be selected for inspection of these types of the structures.

CHAPTER 6

DISCUSSION AND CONCLUSION

In this thesis, the general concept of the guided wave theory was studied for planar structures, wave equations were derived by using the Helmholtz decomposition method and given in the form of two bulk wave velocities in unbounded solid medium. Then using these acoustic properties and applying the boundary conditions on free isotropic elastic plate structure, the Rayleigh Lamb wave equations were derived. The dispersive nature of guided waves were demonstrated, their dispersive characteristics were also analyzed by performing numerical solution of these analytically derived equations.

Following analytical studies, guided waves were investigated with SAFE method for the case of single layer and multilayered system as the aim of this research. The accuracy and capabilities of the SAFE method were studied in planar structures. In the first case study, elastic isotropic plate structure was modelled and analyzed with SAFE method and resulting phase and group velocity dispersion curves were obtained on 2mm titanium plate. The obtained results were then compared with the DISPERSE software programme which solves the wave equations analytically based on GMM. The obtained generalized dispersion curves were in very well agreement with each other on Lamb wave modes. The small errors about (0.62%) on S_0 wave mode and (0.52%) on A_0 wave mode up to 1.4 MHz were observed after applying smallest wavelength assumption. Another observation from this study is that, in order to get more accurate results, higher order polynomial functions could be used or number of elements could be increased up to desired error was achieved for desired applications, while making discretization in SAFE.

Another SAFE analysis was performed to investigate the guided wave propagation in a damped medium. Multi-layered plate configuration consisting of viscoelastic (epoxy) medium sandwiched in between two elastic layers (aluminum) was used. In this case study, the effects of attenuation due to the material damping on dispersion curves were investigated. The solution was employed by adopting hysteretic damping on viscoelastic medium. In this model, material damping was introduced to the

SAFE solution by complex stiffness material matrix. The obtained dispersion curves were compared with the studies available in literature and good agreement on dispersion curves was observed. Mode selection priorities were also discussed by through the attenuation dispersion curve. The obtained attenuation curves for low order modes up to 1 MHz were examined for the purpose of selecting less attenuated wave modes for inspection since the increasing frequency as an example. It was observed from the generalized attenuation curves that, M1 and M3 modes constituted acceptable attenuation levels for inspection, up to 0.66 MHz. Above this frequency, attenuation level of M1 modes increased sharply. In addition to that, the attenuation effects of the viscoelastic layer (damped medium) on dispersion curves were also investigated by increasing the thickness of viscoelastic layer in multilayered system.

To sum up, SAFE method is flexible and powerful tool for obtaining the dispersion features of guided waves when compared with the analytical matrix-based methods. It has a great potential to be used on different types of the waveguides by having the advantages of the using both analytical and FEM methods. It requires far less computational power, compared with the 2D and 3D FEM approaches. On the other hand, the drawbacks of the using SAFE method are that, it should be applied by preparation of special routines and using specialized solvers. Although commercial FEM packages are far less efficient, they have user friendly graphical user interfaces and built-in solvers. Another observation over the SAFE method is that, the obtained eigen value problem solution consists of all computationally possible wave modes. The selection of the propagating wave modes among them is having particular importance and it requires the more computations.

6.1 Future Work

Although this thesis was aimed at to investigate the guided wave problem by making the dispersion analysis on planar waveguides using SAFE method, the proposed method can be used and extended for other types of waveguides like pipes, rods, cylindricals or complex shaped waveguides like rails. The proposed method is flexible enabling easy adoption to the solutions of those types structure. The dispersion analysis could be made by adopting the solution with using 2D discretization on cross-sectional domain of the complex shaped waveguides.

Another future work could be done for anisotropic materials like composites or piezoelectric materials, since the characteristics of these structures was very complex in terms of guided wave analysis. The challenge of making guided wave analysis on composites arise from their nature with multiple layers, possibly with viscoelastic layers and anisotropic behavior. These challenges could be handled with SAFE method by making necessary adjustments. In addition to that, the validation of the obtained results with experiments would be essential for newly developed models.

REFERENCES

- Achenbach, J.D. (1975). "Elastodynamic Theory." *Wave Propagation in Elastic Solids*, 79–121. doi:10.1016/B978-0-7204-0325-1.50008-4.
- Ahmad, Z a B. (2011). "Numerical Simulations of Lamb Waves in Plates Using a Semi-Analytical Finite Element Method (Doctoral Dissertation, Magdeburg, Universität)."
- Alleyne, D.N., and P. Cawley. (1992). "The Interaction of Lamb Waves with Defects." *IEEE Transactions on Ultrasonics, Ferroelectrics and Frequency Control* 39 (3): 381–97. doi:10.1109/58.143172.
- Barshinger, J.N., and J.L. Rose. (2004). "Guided Wave Propagation in an Elastic Hollow Cylinder Coated with a Viscoelastic Material." *IEEE Transactions on Ultrasonics, Ferroelectrics and Frequency Control* 51 (11): 1547–56. doi:10.1109/TUFFC.2004.1367496.
- Bartoli, Ivan, Alessandro Marzani, Francesco Lanza di Scalea, and Erasmo Viola. (2006). "Modeling Wave Propagation in Damped Waveguides of Arbitrary Cross-Section." *Journal of Sound and Vibration* 295 (3–5): 685–707. doi:10.1016/j.jsv.2006.01.021.
- Bartoli, Ivan, Alessandro Marzani, Howard Matt, Francesco Lanza, Erasmo Viola, Structural Engineering, San Diego, and Gilman Drive. (2006). "Modeling Guided Wave Propagation for Structural Health Monitoring Applications." *Proceedings of the SEM IMAC 24th Conference and Exposition on Structural Dynamics*.
- Bernard, A., M. J. S. Lowe, and M. Deschamps. (2001). "Guided Waves Energy Velocity in Absorbing and Non-Absorbing Plates." *The Journal of the Acoustical Society of America* 110 (1). Acoustical Society of America: 186–96. doi:10.1121/1.1375845.
- Birgani, Pezhman Taghipour, Khosro Naderan Tahan, Sina Sodagar, and Mohammad Shishesaz. (2015). "Theoretical Modeling of Low-Attenuation Lamb Wave Modes Generation in Three-Layer Adhesive Joints Using Angle Beam Transducer." *Latin American Journal of Solids and Structures* 12 (3): 461–76.
- Castaings, Michel, and Bernard Hosten. (1994). "Delta Operator Technique to Improve the Thomson–Haskell-method Stability for Propagation in Multilayered Anisotropic Absorbing Plates." *The Journal of the Acoustical Society of America* 95 (4): 1931–41. doi:10.1121/1.408707.
- Cho, Younho, and Joseph L. Rose. (1996). "A Boundary Element Solution for a Mode Conversion Study on the Edge Reflection of Lamb Waves." *The Journal of the Acoustical Society of America* 99 (4). Acoustical Society of America: 2097–2109. doi:10.1121/1.415396.

- Cook, Robert Davis. (2001). *Concepts and Applications of Finite Element Analysis*. John Wiley & Sons.
- Demma, A. (2003). "The interaction of guided waves with discontinuities in structures" (Doctoral dissertation, University of London).
- Drozd, Mickael Brice. (2008). "Efficient Finite Element Modelling of Ultrasound Waves in Elastic Media." (Doctoral dissertation, Imperial College London). <http://ethos.bl.uk/OrderDetails.do?uin=uk.bl.ethos.485413>.
- Fan, Z. (2010). "Applications of guided wave propagation on waveguides with irregular cross-section" (Doctoral dissertation, Imperial College London).
- Finnveden, S. (2004). "Evaluation of Modal Density and Group Velocity by a Finite Element Method." *Journal of Sound and Vibration* 273: 51–75. doi:10.1016/j.jsv.2003.04.004.
- Gao, Huidong. (2007). "Ultrasonic Guided Wave Mechanics for Composite Material Structural Health Monitoring." Source: *Dissertation Abstracts International*, Volume:68-05, The Pennsylvania State University.
- Gavrić, L. (1995). "Computation of Propagative Waves in Free Rail Using a Finite Element Technique." *Journal of Sound and Vibration* 185 (3): 531–43. doi:10.1006/jsvi.1995.0398.
- Gazis, Denos C. (1959a). "Three-Dimensional Investigation of the Propagation of Waves in Hollow Circular Cylinders. I. Analytical Foundation." *The Journal of the Acoustical Society of America* 31 (5): 568–73. doi:10.1121/1.1907753.
- Gazis, Denos C. (1959b). "Three-Dimensional Investigation of the Propagation of Waves in Hollow Circular Cylinders. II. Numerical Results." *The Journal of the Acoustical Society of America* 31 (5). *Acoustical Society of America*: 573–78. doi:10.1121/1.1907754.
- Haskell, N. A. (1953). "The Dispersion of Surface Waves on Multilayered Media." *Bulletin of the Seismological Society of America* 43 (1). *Seismological Society of America*: 17–34.
- Hayashi, Takahiro, Won Joon Song, and Joseph L. Rose. (2003). "Guided Wave Dispersion Curves for a Bar with an Arbitrary Cross-Section, a Rod and Rail Example." *Ultrasonics* 41 (3): 175–83. doi:10.1016/S0041-624X(03)00097-0.
- Juluri, N. (2008). "Inspection of complex structures using guided waves" (Doctoral dissertation, Imperial College London).
- Kamal, Ayman M., Matthieu Gresil, and Victor Giurgiutiu. (2013). "Comparative Study of Several Methods for the Calculation of Ultrasonic Guided Waves in Composites." 54th AIAA/ASME/ASCE/AHS/ASC Structures, Structural Dynamics, and Materials Conference, no. APRIL: 1–21. doi:10.2514/6.2013-1901.

- Knopoff, L. (1964). "A Matrix Method for Elastic Wave Problems." *Bulletin of the Seismological Society of America* 54 (1): 431–38.
- Lamb, H. (1917). "On Waves in an Elastic Plate." *Proceedings of the Royal Society of London. Series A, Containing Papers of a Mathematical and Physical Character (1905-1934)* 20 (21): 114–28. doi:10.1098/rspa.1917.0008.
- Lee, B C, and W J Staszewski. (2003). "Modelling of Lamb Waves for Damage Detection in Metallic Structures: Part II. Wave Interactions with Damage." *Smart Materials and Structures* 12 (5): 815–24. doi:10.1088/0964-1726/12/5/019.
- Lee, Chong Myoung. (2006). "Elastic Waves in Bounded Structures with an Arbitrary Cross-Section." Retrieved from: <https://etda.libraries.psu.edu/catalog/7023>.
- Love, A. E. H. (Augustus Edward Hough). (1944). *A Treatise on the Mathematical Theory of Elasticity*. Dover Publications.
- Lowe, M J S. (1995). "Matrix Techniques for Modeling Ultrasonic-Waves in Multilayered Media." *Ieee Transactions on Ultrasonics Ferroelectrics and Frequency Control* 42 (4): 525–42. doi:10.1109/58.393096.
- Manconi, E., and B. R. Mace. (2007). "Modelling Wave Propagation in Two-Dimensional Structures Using a Wave/Finite Element Technique." *ISVR Technical Memorandum* 966, no. February.
- Mazzotti, M., I. Bartoli, A. Marzani, and E. Viola. (2013). "A Coupled SAFE-2.5D BEM Approach for the Dispersion Analysis of Damped Leaky Guided Waves in Embedded Waveguides of Arbitrary Cross-Section." *Ultrasonics*. doi:10.1016/j.ultras.2013.03.003.
- Moser, Friedrich, Laurence J. Jacobs, and Jianmin Qu. (1999). "Modeling Elastic Wave Propagation in Waveguides with the Finite Element Method." *NDT & E International* 32 (4): 225–34. doi:10.1016/S0963-8695(98)00045-0.
- Mu, Jing, and Joseph L Rose. (2008). "Guided Wave Propagation and Mode Differentiation in Hollow Cylinders with Viscoelastic Coatings." *The Journal of the Acoustical Society of America* 124 (2): 866–74. doi:10.1121/1.2940586.
- Nayfeh, Adnan H., and D. E. Chimenti. (1989). "Free Wave Propagation in Plates of General Anisotropic Media." In *Review of Progress in Quantitative Nondestructive Evaluation*, 181–88. Boston, MA: Springer US. doi:10.1007/978-1-4613-0817123.
- Pavlakovic, Brian, Mike Lowe, David Alleyne, and Peter Cawley. (1997). "Disperse: A General Purpose Program for Creating Dispersion Curves." In *Review of Progress in Quantitative Nondestructive Evaluation*, 185–92. Boston, MA: Springer US. doi:10.1007/978-1-4615-5947-4_24.
- R. Balasubramanyam, D. Quinney, R. E. Challis, C. P. D. Todd. (1996) "A finite-difference simulation of ultrasonic Lamb waves in metal sheets with experimental verification", *Journal of Physics D: Applied Physics* 29 (1) 147–155.

- Rayleigh, Lord. (1885). "On Waves Propagated along the Plane Surface of an Elastic Solid." *Proceedings of the London Mathematical Society* s1-17 (1). Oxford University Press: 4–11. doi:10.1112/plms/s1-17.1.4.
- Rose, Joseph L. (2014). *Ultrasonic Guided Waves in Solid Media*. Cambridge University Press. doi:10.1017/CBO9781107273610.
- Scholte, J.G. (1942), "On the Stoneley Wave Equation," *Proc. Kon. Nederl. Akad. Wetensch.* 45, 20-25, 159-164.
- Simonetti, Francesco. (2003). "Sound Propagation in Lossless Waveguides Coated with Attenuative Materials." *Mechanical Engineering*, no. October: 180.
- Stoneley, R. (1924). "Elastic Waves at the Surface of Separation of Two Solids." *Proceedings of the Royal Society of London A: Mathematical, Physical and Engineering Sciences* 106 (738).
- Thomson, William T. (1950). "Transmission of Elastic Waves through a Stratified Solid Medium." *Journal of Applied Physics* 21 (2). American Institute of Physics: 89–93. doi:10.1063/1.1699629.
- Velsor, Jason Kenneth Van. (2009). "Circumferential Guided Waves in Elastic and Viscoelastic Multilayered Annuli." Doctoral dissertation, The Pennsylvania State University. Retrieved from: <https://etda.libraries.psu.edu/catalog/9498>.
- Viktorov, I a. (1967). "Rayleigh and Lamb Waves : Physical Theory and Applications." New York, New York, Plenum Press. <https://searchworks.stanford.edu/view/602874>.
- Willberg, C., S Duczak, J. M. Vivar-Perez, and Z. A. B. Ahmad. (2015). "Simulation Methods for Guided Wave-Based Structural Health Monitoring: A Review." *Applied Mechanics Reviews* 67 (1): 10803. doi:10.1115/1.4029539.
- Yang, Z., and H. Zhou. (1999). "A Boundary Element Method in Elastodynamics for Geometrically Axisymmetric Problems." *Applied Mathematical Modelling* 23 (6): 501–8. doi:10.1016/S0307-904X(98)10095-1.